The role of AMP-kinase during myogenesis in C2C12 cells

Mohamed Asgar, Nur Farehan Binte

DOCTOR OF PHILOSOPHY

Department of Physiological Sciences

School of Life Science

SOKENDAI (The Graduate University for Advanced Studies)

2016

CONTENTS

ABSTRACT

Myogenesis is a highly coordinated multi-step process that begins with the commitment of progenitor cells, known as myoblasts, to proliferate and subsequently differentiate to form multi-nucleated myotubes. The process of myogenesis is controlled by several myogenic transcription factors that act as terminal effectors of signaling cascades, producing appropriate developmental stage-specific transcripts. For example, MyoD is expressed during the early stage of myogenesis, while myogenin and muscle creatine kinase (MCK) are expressed during the early and late stages of differentiation respectively.

AMP-activated protein kinase (AMPK) plays a key role as a master regulator of cellular energy homeostasis and it exists as heterotrimeric complexes, comprising of the catalytic α subunit and regulatory β and γ subunits. Previous studies have shown that lack of AMPKα2 in skeletal muscle results in lower exercise tolerance and voluntary activity. On the other hand, lack of AMPKα1 is associated with reduced satellite cell activation and impaired muscle regeneration, suggesting an isoform-specific role of AMPK in myogenesis. However, the link between AMPK and myogenesis still remains elusive. Thus, using C2C12 murine myoblast cells lines, I elucidated the isoform-specific roles of AMPK during myogenesis.

Lentiviruses expressing both EGFP and shRNA for AMPKα1, AMPKα2 and both α1- and α2 isoforms (PanAMPK) were infected into intact C2C12 myoblasts to generate stable cell lines. The infected myoblasts were subjected to fluorescence-activated cell

sorting (FACS) to isolate EGFP positive cells that were used for subsequent cultures. shRNAs for AMPKα1 and α2 decreased mRNA abundance of AMPKα1 and α2, respectively, and shRNA for PanAMPK (AMPKα1 plus AMPKα2) decreased both of AMPKα1 and α2. Expression profiles indicated that while AMPKα1 mRNA and protein expressions remained constant, those of AMPKα2 increased during 6 days of differentiation. I examined the cell proliferation rate of the FACS-sorted myoblasts. Selective knockdown of AMPKα1 as well as PanAMPK, but not AMPKα2, resulted in a dramatic reduction of cell proliferation rate, suggesting that AMPKα1 is necessary for cell proliferation of C2C12 myoblasts.

I next studied the effects of isoform-specific depletion of AMPKα1 and α2 on differentiation. At 6 days of differentiation, shAMPKα2 as well as shPanAMPK myotubes were significantly thinner, while shAMPKα1 myotubes were thicker than that of the control. Knockdown of AMPKα1 and PanAMPK significantly decreased the peak expression of myogenin at 72hrs of differentiation. Contrarily, AMPKα2 knockdown resulted in a dramatic reduction in the mRNA expressions of MCK and genes involved in mitochondrial biogenesis including peroxisome proliferator-activated receptor gamma coactivator 1-alpha (PGC-1α). I examined the staining of C2C12 myotubes at 6 days of differentiation with tetramethylrhodamine methyl ester (TMRM), which is a cell-permeant, fluorescent dye that is readily sequestered by active mitochondria. AMPKα2 knockdown reduced TMRM staining in C2C12 cells. These data suggest that AMPKα1 is essential during early-stage differentiation, while AMPKα2 is critical for muscle maturation during the late stage of differentiation. AMPKα1 and α2 reciprocally regulate

the width of C2C12 myotubes during the late stage of differentiation.

In addition to the effects of AMPK on gene expressions, AMPK stimulates fatty acid oxidation and autophagy by phosphorylating acetyl-CoA carboxylase (ACC) and Unc51-like autophagy activating kinase 1 (ULK1), respectively. The results showed that AMPKα1 is the major contributor towards phosphorylation of ACC and ULK1 in C2C12 myotubes.

My findings indicate that AMPKα1 and α2 have distinct roles in myogenic differentiation in C2C12 cells. AMPKα1 is predominantly localised in the cytoplasm while AMPKα2 is present in both nucleus and the cytoplasm. Moreover, a putative nuclear localisation sequence (NLS) has been identified in AMPKα2 but not α1. I discovered that a portion of endogenous AMPKα2 is localised in the nucleus during the late stage of differentiation. To examine the role of AMPKα2 translocation into the nucleus during myogenic differentiation, I overexpressed WT-AMPKα2 and its NLS-mutated form (ΔNLS-AMPKα2) in shAMPKα2 C2C12 cells. AMPK activation by ACIAR (5-Aminoimidazole-4-carboxamide ribonucleotide) or energy deprivation condition (addition of 2-deoxy-D-glucose into low glucose medium) increased the translocation of AMPKα2 in WT-AMPKα2 but not ΔNLS-AMPKα2 myoblasts. I found that WT-AMPKα2 overexpression increased the mRNA abundance of MCK and PGC-1α in shAMPKα2 cells. I also found that while ΔNLS-AMPKα2 overexpression increased the amount of MCK mRNA to a similar extent with that of WT-AMPKα2, it did not increase PGC-1α mRNA expression. The width of shAMPKα2 myotubes was recovered in WT-AMPKα2-expressing cells and partially rescued in ΔNLS-AMPKα2-expressing cells. These results suggest that PGC-1α mRNA

expression, but not MCK expression, could be regulated by AMPKα2 nuclear translocation.

Taken together, my results indicate that AMPKα1 and α2 have distinct roles in myogenic differentiation, with AMPKα1 being necessary during the early stage, while AMPKα2 and its changing subcellular localisation being indispensable during the late stage of differentiation.

INTRODUCTION

Myogenesis is the formation of muscular tissue, during which progenitor cells, known as myoblasts, undergo terminal differentiation and fuse into long, multi-nucleated myotubes. This process, also known as skeletal muscle differentiation, is highly coordinated, occurring in multi-stages in which mononucleated myoblasts first withdraw from the cell cycle in response to extracellular cues, and differentiate into multi-nucleated myotubes that subsequently mature into muscle fibres. The fusion process is characterised by the alignment of myoblast and myotube membranes and this occurs in two stages; primary fusion is defined by myoblast to myoblast fusion, resulting in the formation of nascent myotubes, while secondary fusion results in nuclear accumulation and the growth of the myotube [Abmayr and Pavlath (2012); Hindi et al. (2013)]. During this whole myogenic process, specific marker proteins are expressed at different stages; Paired-box protein (Pax7) maintains a population of quiescent satellite cells, and myoblast determination protein (MyoD), an early differentiation marker, determines the differentiation potential of an activated myoblast and acts in concert with myogenin, a middle stage differentiation marker [Knight and Kothary (2011); Bentzinger et al. (2012); Hindi et al. (2013)]. Muscle creatine kinase (MCK), which is essential for the regulation of energy metabolism in skeletal muscle, is also designated as a late stage differentiation marker [Chamberlain et al. (1985); Johnson et al. (1989)]

Adenosine monophosphate-activated protein kinase (AMPK) is an evolutionarily conserved serine/threonine kinase that functions as a sensor to monitor cellular energy status in response to stresses that consume ATP supplies. It exists as heterotrimeric

complexes, comprising of the catalytic α subunit and regulatory β and γ subunits. In mammals, there are two genes encoding the AMPK α subunit (α1 and α2), two β genes (β1 and β2) and three γ subunit genes (γ1, γ2 and γ3) [Stapleton et al. (1996); Thornton et al. (1998); Cheung et al. (2000); Hardie (2011)]. These seven subunit isoforms could potentially give rise to as many as 12 heterotrimeric combinations; however, in human skeletal muscle, AMPK activity can be accounted for by just three combinations α1β2γ1, α2β2γ1 and α2β2γ3 [Mihaylova and Shaw (2011); Mounier et al. (2015); Ross et al. (2016)].

AMPK is activated in response to stresses that deplete cellular adenosine triphosphate (ATP) supplies. These stressors include low glucose, hypoxia, ischemia, as well as exercise. AMPK can also be pharmacologically activated by 5-Aminoimidazole-4-carboxamide ribonucleotide (AICAR), a cell-permeable precursor to ZMP (AICAR monophosphate), which mimics adenosine monophosphate (AMP). Increased concentrations of AMP and adenosine diphosphate (ADP) will result in their binding to the γ regulatory subunit of AMPK, leading to a conformational change that promotes AMPK phosphorylation and also protects AMPK from dephosphorylation to ensure it remains activated [Hardie (2011); Mihaylova and Shaw (2011); Gowans et al. (2013)]. Phosphorylation of threonine 172 in the activation loop of AMPK is required for AMPK activation, and it has been established that several upstream kinases, such as Liver Kinase B1 (LKB1) and calcium/calmodulin-dependent protein kinase kinase 2 (CAMKK2), directly mediate this event; these upstream kinases are termed as AMPK-activating protein kinases (AMPKK) [Hardie (2011); Mihaylova and Shaw (2011)].

Upon activation, AMPK increases cellular energy levels by inhibiting anabolic energy consuming pathways, such as fatty acid synthesis, protein synthesis, glycogen synthesis etc., and stimulating energy producing catabolic pathways, such as fatty acid oxidation, glucose transport, glycolysis etc. [Hardie (2011); Mihaylova and Shaw (2011); Hardie et al. (2012)]. Muscle contraction during exercise is the main method carried out by the body that can provide the conditions necessary for AMPK activation. Under such conditions, AMP and ADP levels are rapidly increased, leading to AMPK activation and the phosphorylation of target proteins that regulate cell polarity, fatty acid oxidation, mitochondrial biogenesis, as well as autophagy [Hawley et al. (2006); Sriwijitkamol et al. (2007); Egan and Zierath (2013); Lantier et al. (2014)].

AMPKα2 isoform is highly expressed in skeletal muscle, with reports stating that α2-, but not α1-containing complexes, contribute to the activation of AMPK in muscle during contraction [Vavvas et al. (1997)]. AMPKα2 knockdown mice have been reported to decrease voluntary activity, and muscle-specific transgenic mice expressing an inactive AMPKα2D157A mutant (AMPK-dominant negative) showed a significantly lower exercise tolerance [(Mu et al. (2001); Fujii et al. (2007)]. On the other hand, AMPKα1 knock-out (KO) but not AMPKα2 KO has been associated with reduced satellite cell activation and impaired muscle regeneration [Fu et al. (2013a); Fu et al. (2016)]. These results suggest that there is an isoform-specific role of AMPK in muscle function and myogenesis. To date, however, the link between AMPK and myogenesis still remains poorly defined.

Hence, using C2C12 cells, the objective of my study is to elucidate the isoform-specific role of AMPK during myogenesis. C2C12 are murine myoblast cells, which are a subclone of C2 myoblasts, originally obtained from the thigh muscle of C3H mice after a crush injury, and they spontaneously differentiate under low serum conditions [Yaffe and Saxel (1977); Blau et al. (1983); Cheng et al. (2014)]. I found that selective knockdown of AMPKα1, as well as double knockdown of AMPKα1 and AMPKα2 i.e. PanAMPK, resulted in a dramatic reduction of cell proliferation rate, suggesting that AMPKα1 is necessary for cell proliferation of C2C12 myoblasts. In contrast, selective knockdown of AMPKα2, as well as PanAMPK, resulted in a dramatic reduction in MCK gene, as well as some of the genes involved in the modulation of mitochondrial biogenesis. Overall, my results indicate that AMPK plays an important role in myogenic differentiation, with AMPKα1 being necessary during the early stages, while AMPKα2 is indispensable during the late stages of differentiation.

METHODS

Cell culture

Myoblasts

The mouse myoblast C2C12 cell line was obtained from the American Type Culture Collection (ATCC, Manassas, VA). Cells were cultured in Dulbecco's modified Eagle's medium (DMEM) containing glucose at 4500mg/L (Sigma-Aldrich, St. Louis, MO) and were supplemented with 10% heat-inactivated foetal bovine serum (FBS) (Life Technologies, Carlsbad, CA).

Myotubes

When C2C12 cells reached 70-80% confluence, they were first rinsed briefly with phosphate-buffered saline (PBS) [137mM NaCl, 10mM Na_2HPO_4, 2.7mM KCl and 1.76mM KH_2PO_4, pH 7.4)] and then induced to differentiate in DMEM containing glucose at 4500mg/L, supplemented with 2% horse serum (HS) (Life Technologies), for 6 days.

Lentivirus transduction

Short hairpin RNAs (shRNAs) coding the respective sequences for mouse AMPKα1 and AMPKα2 (shPanAMPK), mouse AMPKα1 (shAMPKα1), and mouse AMPKα2 (shAMPKα2), under the control of the mouse U6 gene promoter, were inserted into pFUGW (kindly provided by P. Osten, Cold Spring Harbor Laboratory). The shRNA target sequences were as follows: PanAMPK, 5′-gatgtcagatggtgaattt-3′; AMPKα1, 5′-gtacttaaacccttcagta-3′; AMPKα2, 5′-gaagcgagcgactatcaaa-3′.

Lentiviruses were transduced by co-transfection of Lenti-X 293T human embryonic kidney (HEK) cells (Takara, Shiga, Japan) with vectors encoding the shRNA sequence of interest, the HIV-1 packaging vector Δ8.9 (pΔ8.9) and the gene for the envelope glycoprotein of vesicular stomatitis virus (pVSV-G), using Polyethylenimine (Polysciences, Warrington, PA). Virus particles in culture supernatants were collected by centrifugation at 2,000g x *g* for 5min.

C2C12 myoblasts were seeded in 6-well plates and cultured until 70% confluence, after which 2/3 of the existing medium from each well was replaced by the lentivirus supernatant. The myoblasts were infected for 16hrs and replated onto 100mm tissue culture (TC) dishes where they were cultured for another 24-48hrs. The infected myoblasts were then harvested and re-suspended in ice cold PBS containing 5% FBS and 2μg/ml propidium iodide (PI). The myoblasts were subjected to fluorescence activated cell sorting (FACS) using Cell Sorter SH800 (Sony Corporation, Tokyo, Japan), during which green fluorescence protein (GFP)-positive myoblasts were isolated. The sorted GFP-positive myoblasts were then cultured, after which the expressions for AMPKα1 and AMPKα2 were confirmed by Western blot and real time quantitative PCR (RT-qPCR). Following confirmation, the GFP-positive cells expressing the respective shRNAs for AMPK(s), henceforth termed as shPanAMPK, shAMPKα1 and shAMPKα2 myoblasts (or myotubes), were used for subsequent assays.

All recombinant DNA experiments including production of viral vectors were approved by the relevant committee of the National Institute for Physiological Sciences, and were performed under biosafety level 2 containment for lentivirus.

Mutagenesis: construction of Flag-tagged NLS-mutated AMPKα2 (ΔNLS-AMPKα2) and overexpression of wild type (WT-AMPKα2) and ΔNLS-AMPKα2

Mutagenesis for ΔNLS-AMPKα2 was performed by PCR with *Thermococcus kodakaraensis* plus (KOD+) DNA polymerase (Toyobo, Osaka, Japan) to generate two fragments i.e. Fragment A and Fragment B, using a cDNA for Flag-tagged (NH_2-terminal) mouse wild-type (WT) AMPKα2 as a template. Fragment A contains ATG and FLAG sequences, while Fragment B contains the site-directed mutation in the NLS sequence (-K-**K**-I-R- → -K-**A**-I-R).

The mutagenesis primers for these fragments were as follows:

Fragment A Forward, 5′-CGGGATCCGTCGACACCATGGATTACAAGGACGATGACGACAAG GCTGAGAAGCAGAAGCCGACG-3′; Fragment A Reverse (ΔNLS position), 5′-GGATGTAAAACACACCCCCTCGGATCGCCTTGAAGAGCGTAGGCACGTGCTC-3′; Fragment B Forward (ΔNLS position), 5′-GAGCACGTGCCTACGCTCTTCAAGGCGATCCGAGGGGGTGTG TTTTACATCC-3′; Fragment B Reverse, 5′-GGAATTCGATAATCAACGAGCTAAAGCAGTGA TAAGACTGGCGCAC-3′.

Both fragments were combined by denaturing at 94°C and cooled slowly to 30°C to allow them to anneal at the ΔNLS primer positions. KOD+ DNA polymerase (Toyobo) was then added to the PCR reaction to fill in the gaps. The PCR reaction was heated up slowly to 72°C, preceding the addition of Fragment A Forward and Fragment B Reverse flanking primers for amplification. Mutation was confirmed by DNA sequencing using the Applied Biosystems 3130xl Genetic Analyser (Thermo Fisher Scientific, Rockford, IL).

WT-AMPKα2 and ΔNLS-AMPKα2 DNA inserts were ligated into pFU/W lentiviral vector and then transformed into Stbl3 competent cells (Life Technologies). Following DNA purification, the overexpression plasmids were co-transfected with pΔ8.9 and pVSV-G plasmids into Lenti-X 293T cells in order to transduce lentiviruses expressing WT-AMPKα2 and ΔNLS-AMPKα2. These lentiviruses were used to infect C2C12 control and shAMPKα2 myoblasts for 16hrs, after which they were replated onto 100mm TC dishes where they were cultured until 70-80% confluence before differentiation was induced for 6 days.

Growth curve assay

C2C12 myoblasts from the four different cell lines i.e. control, shPanAMPK, shAMPKα1 and shAMPKα2 were seeded in 12-well plates at a density of 1 X 10^4 and then cultured up to 72hrs. During the 72hr period, the cells were trypsinised, collected and counted using a haemocytometer, at 24-hr intervals. Assay was performed in triplicates.

Transfection and stimulation with AMPK activator and energy deprivation condition

Transient transfection of pCAGGS vector expressing Flag-tagged WT-AMPKα2 or Flag-tagged ΔNLS-AMPKα2 (2 μg per well respectively) into C2C12 myoblasts cultured in 6-well plates was performed with Lipofectamine 2000 Reagent (Life Technologies) in Opti-MEM (Life Technologies) for 4 hrs, after which the media was replaced with DMEM supplemented with 10% FBS. Transfected myoblasts were stimulated with 0.5mM of 5-Aminoimidazole-4-carboxamide ribonucleotide (AICAR) (Toronto Research Chemicals, Toronto, ON) and DMEM containing glucose at 1000mg/L (Sigma-Aldrich), supplemented

with 21.3mM of 2-deoxy-D-glucose (2DG) (Sigma-Aldrich). Following the respective stimulations, the myoblasts were subjected to immunofluorescence staining.

Immunofluorescence staining

C2C12 myoblasts, as well as myotubes, were grown on cover slips and then fixed with 4% paraformaldehyde for 20min at room temperature. The myoblasts/myotubes were then permeabilised with cold acetone on ice for 20min and treated with 2% bovine serum albumin and 5% foetal bovine serum in phosphate-buffered saline for 1hr. The myoblasts/myotubes were subsequently incubated with rabbit polyclonal antibodies for AMPKα2 and FLAG overnight at 4^{o}C, and Alexa Fluor 488-labelled goat antibodies for rabbit immunoglobulin G (IgG) (Cat. A11008, 1:500; Life Technologies). Nuclei were visualised by mounting slides with 4', 6-diamidino-2-phenylindole (DAPI) Fluoromount-G (Southern Biotech, Birmingham, AL). Fluorescence of Alexa Fluor 488 and DAPI were observed under fluorescence microscope (DMI4000B; Leica Microsystems, Warzlar, Germany). All primary antibodies used for immunofluorescence staining are listed in Table II.

Measurement of myotube diameter

The myotube diameters of control, shPanAMPK, shAMPKα1 and shAMPKα2 cell lines were determined after 6 days of differentiation, using a fluorescence microscope (DMI4000B; Leica Microsystems) under phase contrast, 200X magnification. Each group was cultured in 100mm TC dishes and an image was captured for seven independent fields. Selection criteria for a differentiated myotube was adhered, in that it must contain

at least three nuclei in a single alignment and that it should have a length of more than three myoblasts. Three short-axis measurements were taken along the length of a given myotube diameter and the average was calculated. A total of 50 myotubes were measured from each 100mm TC dish. Three independent experiments were performed.

Nuclear localisation of AMPKα2

C2C12 myoblasts were transfected with Flag-tagged WT-AMPKα2 or Flag-tagged ΔNLS-AMPKα2 plasmids and subsequently subjected to AICAR (Toronto Research Chemicals) and low glucose-2DG stimulations, and followed by immunofluorescence staining with FLAG polyclonal antibody (refer to Table 2), Alexa Fluor 488 (Life Technologies) and DAPI (Southern Biotech). Cells with at least 50% overlap between FLAG and DAPI fluorescence were counted as having nuclear translocation, whereas cells with no overlap between FLAG and DAPI fluorescence were counted as negative nuclear translocation. A total of 500 transfected cells from six independent fields were counted for each group.

Tetramethylrhodamine methyl ester (TMRM) staining

C2C12 myotubes that were differentiated for 6 days, were subjected to TMRM staining. 20nM TMRM was added to the myotubes cultured in differentiation medium and then incubated at 37^{o}C for 30min, after which they were washed once with PBS. The myotubes were then overlaid with PBS for live-cell imaging under fluorescence microscope (DMI4000B; Leica Microsystems). Exposure time was performed manually to ensure that the fluorescence intensity is uniform for control, shPanAMPK, shAMPKα1 and shAMPKα2 cell lines. TMRM and EGFP images were analysed in ImageJ software

(National Institutes of Health, Bethesda, MD) to determine the level of fluorescence in a fixed region of interest (ROI) [Gavet and Pines (2010); McCloy et al. (2014)]. A total of 20 independent ROIs were selected from each TMRM and EGFP image.

RNA extraction, RT-PCR and quantitative PCR

Total RNA was extracted from both C2C12 myoblasts and myotubes with Trizol Reagent (Life Technologies). 500ng of the purified RNA were subjected to reverse transcription (RT) with avian myeloblastosis virus (AMV) reverse transcriptase and an oligo (dT) primer (Takara). FLAG-tagged AMPKα2 transcripts (Flag-tagged WT-AMPKα2 and Flag-tagged ΔNLS-AMPKα2) were detected by PCR with ExTaq (Takara) and Veriti 96-well Thermal Cycler (Life Technologies). RT-qPCR was performed using the StepOne Real-Time PCR system (Life Technologies) with 1 µl of 1:5 dilution of the resulting cDNA and SYBR Premix Ex Taq II (Tli RNaseH Plus) (Takara). All reactions were analysed in duplicates. Data were normalised to the signal obtained using primers that amplify the 36B4 transcripts, based on comparative CT method for relative quantitation of gene expression. All primer sequences are listed in Table I.

Protein extraction and Western blotting

C2C12 myoblasts cultured for 48hr, as well as C2C12 myotubes differentiated for 6 days, were harvested and lysed in buffer containing 20mM Tris (pH 7.4), 5mM EDTA (pH 8.0), 10mM sodium pyrophosphate, 1% Triton X-100, with protease and phosphatase inhibitor cocktails (Sigma-Aldrich and Calbiochem, San Diego, CA, respectively). Protein concentrations of cell lysates were determined by bicinchoninic acid (BCA) assay (Pierce,

Thermo Fisher Scientific). Cell lysates were subjected to SDS-polyacrylamide gel electrophoresis, and the separated proteins were transferred onto a polyvinylidene difluoride membrane. After blocking in Tris-buffered saline [(50mM Tris-HCl (pH7.5), 150mM NaCl and 0.1% Tween 20)] containing 5% skim milk for 2hr at room temperature, the membranes were probed with specific primary antibodies. Immunoreactive protein bands were detected with goat anti-rabbit horseradish peroxidase-conjugated secondary antibody (Santa Cruz Biotechnology, Santa Cruz, CA) and enhanced chemiluminescence reagents (GE Healthcare, Buckinghamshire, United Kingdom). Protein bands were captured on ImageQuant LAS 1000 mini (GE Healthcare) and processed using ImageJ software (National Institutes of Health). All primary antibodies used for Western blotting are listed in Table II. β- actin was used as a loading control since its expression was comparatively similar throughout the stages in myogenesis (see RESULTS).

Immunoprecipitation

Cell lysates (200µg) prepared from above were incubated with Buffer A [20mM Tris-HCl (pH7.4), 1mM EDTA (pH 8.0), 50mM NaCl, 10mM sodium pyrophosphate, 250mM sucrose, protease and phosphatase inhibitor cocktails (Sigma-Aldrich and Calbiochem respectively)], AMPKα1 or AMPKα2 antibodies (in-house produced) and Protein A/G Sepharose mix (GE Healthcare) at 4^{o}C overnight. The resulting Protein A/G Sepharose beads were separated by centrifugation, washed twice with Buffer A and twice more with cold PBS, after which they were subjected to Western blotting.

Statistical analysis

Data are presented as means ± s.e.m. Statistical comparisons among multiple groups were performed by analysis of variance (ANOVA) followed by Tukey-Kramer's post hoc test. Statistical analysis between two groups were performed by unpaired or paired Student's *t* test (two-tailed). A *P* value of <0.05 was considered statistically significant. Comparisons of mean diameter, as well as AMPKα2 mRNA amounts in shAMPKα2-expressing myotubes overexpressed with WT-AMPKα2 and ΔNLS-AMPKα2, were performed after logarithmic conversion.

RESULTS

Knockdown of AMPKα1 delays cell proliferation rate

Figures 1A-D show the results of FACS for EGFP-positive control, shPanAMPK, shAMPKα1, and shAMPKα2 myoblasts, respectively. More than 95% of the sorted myoblasts were positive for EGFP. The number of these myoblasts at each time point during culture revealed that shPanAMPK and shAMPKα1 myoblasts had a significantly slower proliferation rate, compared with that of EGFP-positive control myoblasts (Figure 1E and F). In contrast, the proliferation of shAMPKα2 myoblasts was similar to the control myoblasts at all time points (Figure 1F, yellow line). These results suggest that AMPKα1 is necessary for cell proliferation in C2C12 myoblasts.

AMPKα1 protein expression remains constant while that of AMPKα2 increases during differentiation

I examined AMPKα1 and α2 mRNA abundance in control, shPanAMPK, shAMPKα1 and shAMPKα2 myoblasts and myotubes (Figure 2A and B). Cells collected were myoblasts at 24hr, and myotubes at 24hr, 72hr and 6 days after replacement with differentiation medium. AMPKα1 was highly expressed in 24hr myoblasts; and its expression was slightly decreased in myotubes at 24hr, 72hr and 6 days (Figure 2A). mRNA abundance of AMPKα1 was significantly decreased in shPanAMPK and shAMPKα1 cell lines, while its expression in shAMPKα2 cell line was similar to that of control. Contrary to the expression of AMPKα1, AMPKα2 mRNA abundance was significantly higher in myotubes

than that in myoblasts (Figure 2B). In myotubes, the amount of AMPKα2 mRNA was significantly decreased in shPanAMPK and shAMPKα2 myotubes. shAMPKα1 myotubes slightly decreased the amount of AMPKα2 mRNA at 24hr, but not at 72hr or 6 days. The expression of AMPKα2 mRNA in myoblasts was not affected by shPanAMPK, shAMPKα1 or shAMPKα2, suggesting a very low expression of AMPKα2 in myoblasts.

I also examined the protein expressions of total AMPK, AMPKα1 and AMPKα2 in control, shPanAMPK, shAMPKα1 and shAMPKα2 myotubes (Figure 2C). AMPKα1 protein content in both control and shAMPKα2 myotubes remained constant throughout the 6 days of differentiation, while that of shPanAMPK and shAMPKα1 was almost diminished. In contrast, AMPKα2 protein content increased progressively during the 6 days of differentiation. AMPKα2 protein contents of shPanAMPK and shAMPKα2 myotubes were selectively inhibited at all time points. The protein expression, attributed by the changes in both AMPKα1 and AMPKα2 expressions, could be reflected in the immunoblot for total AMPKα. Protein expression of total AMPKα appears to be mainly reflected by the protein amount of AMPKα1. β- actin was comparatively similar throughout the stages in myogenesis. These results suggest that AMPKα1 protein expression remains constant while that of AMPKα2 increases during differentiation.

AMPKα1 and α2 reciprocally regulate the width of C2C12 myotubes

AMPK activation during conditions of energetic stress is thought to act as a negative regulator of protein synthesis and may therefore modulate skeletal muscle mass and hypertrophy [Bolster et al. (2002); Nader et al. (2002)]. I wondered if inhibiting AMPKα activity would have any profound effect on the phenotypes of differentiated myotubes. I captured images of control, shPanAMPK, shAMPKα1 and shAMPKα2 myotubes after 6 days of differentiation. Control myotubes were properly arranged, representing singly aligned nuclei. In contrast, shPanAMPK and shAMPKα2 myotubes were relatively thin, while shAMPKα1 myotubes appeared to be thicker than of control myotubes (Figure 3A).

I measured the width of individual myotubes for the aforementioned cell lines after 6 days of differentiation. Figure 3B shows a representative measurement of the width of individual myotubes. Three short-axis measurements were taken along the length of a given myotube diameter and the average was calculated. A total of 50 myotubes were measured from each 100mm TC dish, and three independent experiments were performed. Selection criteria was adhered, in that it must contain at least three nuclei in a single alignment and that it should have a length of more than three myoblasts. Figure 3C (Histogram) and Figure 3D (cumulative number of cells versus cell diameter) revealed that the width of both shPanAMPK and shAMPKα2 myotubes was shifted leftward compared with the control, while that of shAMPKα1 myotubes was shifted rightward. Mean width (μm) of each group was as follows: Control, 103.0 ± 2.3; shPanAMPK, 72.8 ± 1.6 ($P < 0.05$ vs control), shAMPKα1, 140.8 ± 4.3 ($P < 0.05$ vs control); shAMPKα2, 83.3 ± 2.2 ($P < 0.05$ vs control). The width (μm) at 50% cumulative cell

numbers was also as follows: Control, 98.3; shPanAMPK, 72.0, shAMPKα1, 131.2; shAMPKα2, 78.6. Thus, AMPKα1 knockdown increased but AMPKα2 knockdown decreased the width of C2C12 myotubes.

AMPKα1 is important during the early stage while AMPKα2 is necessary during the late stage of myogenesis

I assessed the mRNA expression of myogenic markers in control myoblasts and myotubes. MyoD, Myogenin and MCK are designated as early, middle and late stage differentiation markers, respectively (Figure 4A) [Chamberlain et al. (1985); Johnson et al. (1989); Knight and Kothary (2011); Bentzinger et al. (2012); Hindi et al. (2013)]. Figure 4B showed that the mRNA abundance for MyoD remained constant throughout myogenesis, while myogenin was expressed in myotubes but not myoblasts, reaching its peak at 72hr and then declined by the 6^{th} day of differentiation (Figure 4C). MCK mRNA was also expressed solely in myotubes, reaching its peak at 6 days (Figure 4D).

I examined whether the mRNA abundance of these myogenic markers would also be affected by shPanAMPK, shAMPKα1 and shAMPKα2. MyoD mRNA abundance in 24hr myotubes was not significantly different among the cell lines compared with control myotubes (Figure 4E). Myogenin mRNA at 72hr was supressed by both shPanAMPK and shAMPKα1, while shAMPKα2 did not suppress the mRNA amount significantly (Figure 4F). Thus, AMPKα1 mostly regulates myogenin expression. In contrast, MCK mRNA expression at 6 days of differentiation was significantly decreased in both shPanAMPK

and shAMPKα2 myotubes, but not shAMPKα1 myotubes (Figure 4G). These results suggest that while AMPKα1 is important during the early stage of myogenesis (the expression of myogenin as well as cell proliferation of myoblasts), AMPKα2 is necessary for muscle maturation during the late stage of differentiation.

Knockdown of AMPKα2 down-regulated mRNA expressions of genes involved in mitochondrial biogenesis and caused a reduction in TMRM staining

AMPK stimulates mitochondrial biogenesis through a PGC-1α –dependent transcription. PGC-1α is a co-transcriptional regulation factor that induces mitochondrial biogenesis by activating nuclear respiratory factor 2 (NRF2), mitochondrial transcription factor A (Tfam) and mitochondrial transcription factor B2 (TFB2M) [Irrcher et al. (2008); Ventura-Clapier et al. (2008)]. To examine the individual contributions of AMPKα1 and AMPKα2 towards mitochondrial biogenesis, I performed RT-qPCR on control, shPanAMPK, shAMPKα1 and shAMPKα2 myotubes at 6 days of differentiation. I found that knockdown of AMPKα2 but not AMPKα1 led to the down-regulation of PGC-1α and TFB2M mRNA amounts (Figure 5A and B). AMPKα2 knockdown also tended to decrease Tfam and NRF2 mRNA abundance (Figure 5C and 5D). shPanAMPK showed a reduction in those mRNA amounts, but the effects were not statistically significant.

TMRM is a cell-permeant, fluorescent dye that is readily sequestered by active mitochondria. shPanAMPK and shAMPKα2 myotubes demonstrated a subdued TMRM staining compared with control and shAMPKα1 myotubes at 6 days of differentiation

(Figure 5E and F). This outcome, along with the RT-qPCR results, suggest that lack of AMPKα2 could inhibit mitochondrial biogenesis.

AMPKα1 is the major contributor towards phosphorylation of ACC and ULK1

In addition to the gene expression, activation of AMPK induces the phosphorylation (pACC) of acetyl Co-A carboxylase (ACC) (serine 79 for ACC1 and serine 212 for ACC2) and promotes fatty acid oxidation and ATP production in the mitochondria [Fullerton et al. (2013)]. AMPK also regulates autophagy, which is initiated by phosphorylating the autophagy-initiating kinase ULK1 on serine 555 (pULK1) [Bach et al. (2011); Alers et al. (2012)]. I examined the individual contributions of AMPKα subunits towards ACC and ULK1 phosphorylation at 6 days of differentiation (Figure 6A). Control and shAMPKα2 myotubes showed a high level of AMPK phosphorylation (pAMPK). In contrast, there was a lesser extent of pAMPK in both shAMPKα1 and shPanAMPK myotubes. shAMPKα1 and shAMPKα2 myotubes also reciprocally increased AMPKα1 and α2 protein content. These results suggest that while AMPKα1 is the major contributor towards pAMPK, the activities of AMPKα1 and α2 are increased in compensation for the absence of either subunit. Analysis of pAMPKα1 and α2 by specific immunoprecipitation showed that both AMPKα1 and α2 are phosphorylated at 6 days of differentiation (Figure 6B and C).

Next, I examined pACC and pULK1 in those cell lines at 6 days of differentiation (Figure 6D and E). Control and shAMPKα2 myotubes showed a high level of pACC and pULK1. In contrast, shAMPKα1 and shPanAMPK myotubes had a much lesser extent of

pACC and pULK1. These results suggest that AMPKα1 could be the major contributor towards the activity of ACC and ULK1 in C2C12 myotubes. However, I also observed that shAMPKα2 and shPanAMPK myotubes change the total amount of ACC and ULK1 respectively, compared with control and shAMPKα1. Thus, AMPKα2 may regulate the protein expression of ACC and ULK1 in C2C12 myotubes.

AMPKα2 translocates to the nucleus upon activation

Previous studies have shown that AMPKα1 and AMPKα2 have different subcellular locations; in skeletal muscle, AMPKα2 appears to be more enriched in the nucleus, while AMPKα1 is mostly localised to the cytoplasm [Salt et al. (1998); McGee et al. (2003); Ross et al. (2016)]. Furthermore, a putative nuclear localisation sequence (NLS) was identified in AMPKα2, but not in AMPKα1 [Suzuki et al. (2007)]. Hence, I examined whether AMPKα2 localises in the nucleus during myogenesis. Immunofluorescence analysis of endogenous AMPKα2 in C2C12 control cells revealed that AMPKα2 expression gradually increased during differentiation, with an increased AMPKα2 in the nucleus (Figure 7A).

I next investigated whether AMPKα2 would translocate to the nucleus upon activation, dependent on the nuclear localisation signal, as previously reported [Suzuki et al. (2007)]. I generated a FLAG-tagged WT-AMPKα2 and FLAG-tagged ΔNLS-AMPKα2 construct, which had a point mutation in its nuclear localisation signal (Figure 7B), and transiently transfected those constructs into C2C12 control myoblasts. In the control without stimulant, FLAG expression remained in the cytoplasm in both WT-AMPKα2 and

ΔNLS-AMPKα2 transfected myoblasts. However, both AICAR and low glucose plus 2DG stimulations increased nuclear localisation of WT-AMPKα2 but not its ΔNLS-AMPKα2 mutant (Figure 7C). I quantified the number of cells containing FLAG protein that had localised in the nucleus. Although about 95% of cells had WT-AMPKα2 localised in the cytoplasm without stimulation, about 40% and 50% had a partly translocated AMPKα2 upon stimulation with AICAR and low glucose plus 2DG, respectively (Figure 7D and E). In contrast, cells transfected with ΔNLS-AMPKα2 remained in the cytoplasm upon stimulation by either (Figure 7D and E).

Expression of WT-AMPKα2 but not ΔNLS-AMPKα2 increases the width of shAMPKα2 cells

I explored the role of AMPKα2 nuclear translocation during myogenic differentiation in control and shAMPKα2 cells that had been overexpressed with WT-AMPKα2 and ΔNLS-AMPKα2 plasmids, and subsequently differentiated for 6 days. There was no apparent phenotypic difference among the control myotubes overexpressed with empty, WT-AMPKα2 and ΔNLS-AMPKα2 vectors (Figure 8A). However, shAMPKα2 myotubes overexpressed with WT-AMPKα2 recovered the width of shAMPKα2 myotubes (Figure 8B). In contrast, overexpressing its ΔNLS mutant resulted in an intermediary phenotype, with the presence of thin and thick myotubes (Figure 8B).

Overexpression of WT-AMPKα2 and its ΔNLS mutant had no apparent effect on AMPKα1 mRNA (Figure 8C) as well as protein expression (Figure 8E) in either the control

or shAMPKα2 myotubes, while shAMPKα2 myotubes tended to decrease AMPKα1 mRNA abundance (Figure 8C). In contrast, shAMPKα2 myotubes significantly decreased total AMPKα2 mRNA abundance (Figure 8D), as shown in Figure 2B. While expression of WT-AMPKα2 and its ΔNLS mutant did not change the total AMPKα2 mRNA abundance (endogenous plus mutated AMPKα2) in the control myotubes (Figure 8D), overexpression of WT-AMPKα2 and its ΔNLS mutant increased the mRNA (Figure 8D) as well as protein (Figure 8E) amount of AMPKα2 in shAMPKα2 myotubes. Protein expression of total AMPKα2 did not differ between myotubes overexpressed with WT-AMPKα2 and ΔNLS-AMPKα2 in either control or shAMPKα2 myotubes (Figure 8E). Expression of WT-AMPKα2 and ΔNLS-AMPKα2 was confirmed with the increased FLAG mRNA expression in the control and shAMPKα2 myotubes (Figure 8F). It was not known why overexpression of WT-AMPKα2 and ΔNLS-AMPKα2 did not alter the AMPKα2 mRNA expression in control myotubes, although its protein expression was increased (Figure 8D and E).

Overexpression of WT-AMPKα2 recovered MCK and PGC-1α expression and the effect on PGC-1α expression was dependent on its nuclear localisation signal

My results indicated that shAMPKα2 knockdown led to a significant reduction in MCK and PGC-1α mRNA expressions, underlining the importance of the α2 subunit during the late stages of differentiation. Therefore, I sought to determine whether overexpression of WT-AMPKα2 and ΔNLS- AMPKα2 would recover MCK and PGC-1α expressions in shAMPKα2 myotubes. I found that overexpression of WT-AMPKα2 increased MCK and

PGC-1α mRNA expressions in shAMPKα2 myotubes, compared to those with empty vector (Figure 8G and H). I also found that although overexpression of ΔNLS-AMPKα2 increased the amount of MCK mRNA to a similar extent with that of WT-AMPKα2 (Figure 8G), it did not increase PGC-1α mRNA expression (Figure 8H). These results suggest that PGC-1α mRNA expression, but not MCK expression, could be regulated by AMPKα2 nuclear translocation.

DISCUSSION

In the present study, I found that AMPKα1 and α2 have distinct roles in myogenic differentiation, with AMPKα1 being necessary during the early stage, while AMPKα2 and its changing subcellular localisation being indispensable during the late stage of differentiation. My results indicate that selective knockdown of AMPKα1 resulted in a dramatic reduction of cell proliferation. Knockdown of AMPKα1 also decreased myogenin gene expression and phosphorylation of ACC and ULK1. In contrast, knockdown of AMPKα2 resulted in a dramatic reduction in MCK gene expression, a late stage marker of muscle differentiation, as well as some of the genes involved in mitochondrial biogenesis such as PGC-1α. Nuclear translocation of AMPKα2 was necessary for PGC-1α mRNA expression, while MCK expression was independent of the translocation. These results suggest that AMPKα1 and α2 have crucial roles during myogenesis of C2C12 cells through multiple downstream signalling pathways.

I have shown that reduced AMPKα1 expression dramatically attenuated cell proliferation in C2C12 myoblasts, highlighting the necessity of the α1 subunit in promoting cell growth of myoblasts. This is consistent with a previous report showing that lack of AMPKα1 reduces proliferation and myogenic capacity of satellite cells during muscle regeneration [Fu et al. (2016)]. Recent studies also revealed that knockdown of AMPKα1 but not AMPKα2 reduced myogenin expression and myogenic differentiation of C2C12 cells through histone deacetylase 5 (HDAC5) phosphorylation [Fu et al. (2013a); Fu et al. (2013b)]. Moreover, AMPKα1 has been reported to directly control hepatocyte proliferation by regulating cyclin A2 expression, which is tightly synchronised with the

progression of the cell cycle [Merlen et al. (2014)]. Thus, AMPKα1 could behave as an important effector in controlling cell proliferation.

AMPK is well known to increase fatty acid oxidation through inhibition of ACC by direct phosphorylation of Ser79 (in ACC1), consequently inhibiting malonyl-CoA production, thereby allowing carnitine palmitoyltransferase (CPT1) to promote long-chain acyl-CoA entry into mitochondria in order to undergo β-oxidation and produce ATP [Winder et al. (1997); Towler and Hardie (2007)]. AMPK is also known to trigger autophagy by directly phosphorylating ULK1 [Egan et al. (2011); Kim et al. (2011)]. I evaluated the individual contributions of AMPKα isoforms towards phosphorylation of ACC and ULK1. I found that phosphorylation of ACC (Ser79) and ULK1 (Ser555) was severely reduced in shAMPKα1 myotubes, underlining AMPKα1 as the major contributor towards promoting fatty acid oxidation and autophagy in C2C12 cells.

A recent study revealed that upon glucose starvation, activated AMPK phosphorylates glyceraldehyde 3-phosphate dehydrogenase (GAPDH) at Ser122 in the cytoplasm, promoting translocation of GAPDH into the nucleus where it directly interacts with and activates Sirt1, thereby initiating autophagy via translocation of Atg8 (LC-3 in mammals) from nucleus to cytoplasm [Chang et al. (2015)]. AMPK also stimulates autophagy by inhibiting mammalian target of rapamycin (mTOR) activity via phosphorylation of tuberous sclerosis 2 (TSC2) [Mihaylova and Shaw (2011)]. Inhibition of mTOR activity by AMPK appears to be mediated by AMPKα1 in some cell lines [Mounier et al. (2009); Lee et al. (2010a); Lee et al. (2010b)]. However, it is not known whether cell proliferation and phosphorylation of ACC and ULK1 in C2C12 cells are

regulated by AMPKα1 specifically or simply due to the high expression of AMPKα1 compared with AMPKα2. Exercise and leptin have been shown to preferentially activate AMPKα2 but not AMPKα1 in skeletal muscle *in vivo*, stimulating phosphorylation of ACC and fatty acid oxidation in the tissue [Minokoshi et al. (2002); Viollet et al. (2009)]. Further experiments are necessary to clarify whether AMPKα1 and α2 are dispensable for cell proliferation, fatty acid oxidation and autophagy in C2C12 cells.

In the present study, I found that shAMPKα1 resulted in a significant increase in the width of myotubes. In contrast, shPanAMPK and shAMPKα2 myotubes decreased the width compared with the control. These results suggest that AMPKα1 and α2 reciprocally regulate cell diameter of C2C12 myotubes. Given that shPanAMPK and shAMPKα2 myotubes are similarly thinner than that of control, the hypertrophic action of shAMPKα1 might be due to a compensatory increase in AMPKα2 expression (Figure 6A). In support of my finding, a previous study showed that AMPKα1 KO primary cultured myotubes exhibited larger cell size compared with control cells [Mounier et al. (2009)]. An age-related elevation in AMPK phosphorylation is strongly correlated with the attenuated hypertrophic response observed with age in overloaded fast-twitch muscle [Thomson and Gordon (2005)]. On the other hand, AMPKα2 has been shown to be the most prevalent isoform in skeletal muscle in maximal exercise capacity and its loss lowers exercise tolerance, as well as decreases voluntary activity in mice [Fujii et al. (2007)]. Hence, my results suggest that AMPKα1 and α2 regulate muscle volume in reciprocal manners: AMPKα2 increases the width of C2C12 cells while AMPKα1 inhibits it.

The effect of AMPKα2 may partly be associated with the stimulatory effects on the gene expressions involved in mitochondrial biogenesis and energy homeostasis, including PGC-1α and MCK. My important finding is that AMPKα2 knockdown significantly affected the differentiation potential in C2C12 myotubes towards the later stage, resulting in a drastic decline in MCK mRNA expression and some of the genes involved in mitochondrial biogenesis such as PGC-1α. My data showed a time-dependent expression of AMPKα2, with its protein levels increasing progressively during the late stages of differentiation. Knockdown of AMPKα2 not only led to the down-regulation of PGC-1α and TFB2M, but also a subdued TMRM staining compared with control myotubes. Forced expression of WT-AMPKα2 was able to rescue the decline in MCK and PGC-1α expression in shAMPKα2 myotubes. I also found that nuclear translocation of AMPKα2 is necessary for PGC-1α but not MCK gene expression in C2C12 myotubes.

Activation of AMPK has been shown to increase mitochondrial biogenesis in skeletal muscle through PGC-1α [Zong et al. (2002); Rohas et al. (2007); Fulco and Sartorelli (2008)]. In humans, acute bout of exercise enhances the nuclear localisation of AMPKα2 [McGee et al. (2003)] and PGC-1α gene expression in muscle [Vissing et al. (2008)]. Muscle-specific deletion of either AMPK or PGC-1α leads to a reduction in mitochondrial biogenesis and exercise intolerance [Zong et al. (2002); Reznick and Shulman (2006); Fulco and Sartorelli (2008)]. While the mechanisms underlying AMPK dependent mitochondrial biogenesis have yet to be fully elucidated, it can be postulated that they might rely on the ability of nuclear AMPKα2 complexes to directly

phosphorylate transcriptional factors and/or co-regulators, to stimulate gene expression of PGC-1α.

Recent study showed that activated AMPK stimulates some gene transcriptions through phosphorylation of histone H2B on Ser36. Mouse embryonic fibroblasts (MEFs) expressing a mutant $H2B^{S36A}$ blunted the induction of stress-related genes upregulated by AMPK, including *p21* and *cpt1c* [Bungard et al. (2010)]. It is also reported that exercise stimulates the phosphorylation of class IIa histone deacetylases (HDACs) and leads to nuclear export, thereby removing their transcriptional repressive function [McGee et al. (2009)]. A previous study also revealed that AMPK stimulates phosphorylation of cAMP response element-binding protein (CREB) at the same site as cAMP-dependent protein kinase (PKA) in cultured cells [Thomson et al. (2008)]. Another study demonstrated that pharmacological activation of AMPK stimulates PGC-1α gene expression through the GATA/Ebox binding site in the promoter region [Irrcher et al. (2008)]. Further experiments are necessary to explore how AMPKα2 regulates PGC-1α and MCK gene expression and mitochondrial function.

Previous studies on isoform composition of AMPK complexes in human skeletal muscle revealed that only 3 of the 12 theoretically possible heterotrimeric combinations i.e. α1β2γ1, α2β2γ1 and α2β2γ3 account for AMPK activity in that tissue [Birk and Wojtaszewski (2006); Mounier et al. (2015); Ross et al. (2016)]. In a preliminary study (data not shown), I found that β1 and γ2 mRNA are highly expressed in C2C12 myoblasts, suggesting that α1/ β1/ γ2 combination is essential for the onset of myogenesis. By contrast, β2, γ1 and γ3 mRNA are almost undetectable in C2C12 myoblasts but are highly

expressed in matured myotubes, a pattern that is similar to α2 expression in my present study, as well as in other *in vivo* studies [Mahlapuu et al. (2004); Wojtaszewski et al. (2005); Birk and Wojtaszewski (2006)]. This suggests that heterotrimeric assembly of α2 with β2 and γ1/ γ3 isoforms, is crucial during the late stages of myogenic differentiation. However, further investigation is necessary to ascertain the changing expression profile of AMPK subunit isoforms in differentiating C2C12 cells. It would also be interesting to determine the functional significance of different AMPK isoform combination in relation with their subcellular localisation during myogenesis.

To reiterate, my data demonstrate that AMPKα1 is necessary for the phosphorylation of ACC and ULK1; this, in turn, could mediate the upregulation of fatty acid oxidation and autophagy respectively (Figure 9). In addition, AMPKα1 is also important for promoting cell proliferation in C2C12 myoblasts. On the other hand, AMPKα2 is essential for the up-regulation of MCK and PGC-1α expressions. In parallel, while nuclear localisation of AMPKα2 is necessary for up-regulating PGC-1α expression, this is not necessary for MCK gene expression. Those effects of AMPKα2 may be associated with the width of C2C12 myotubes. Overall, my current findings point to multiple roles of AMPK during myogenesis; α1 isoform being critical during cell proliferation and the initial stage of myogenesis, while α2 isoform and its subcellular localisation being indispensable for the progression to mature myotubes.

ACKNOWLEDGEMENTS

First and foremost, I would like to extend my utmost gratitude to Professor Yasuhiko Minokoshi for accepting me into the lab in spite of the dire circumstances, as well as for his immense patience, continuous encouragement and invaluable insights throughout my time here in this lab. I would also like to express my deepest and sincere appreciation to Assistant Professor Shiki Okamoto for being such an awesome and effective mentor, and for being so supportive and generous with his time in providing countless hours of discussion every week since I joined the lab.

Next, I would like to express my gratitude to my past mentors, Assistant Professor Takuya Sasaki (Lab Chem Pharmacol, University of Tokyo) and Dr. Akio Sekigawa (Carl Zeiss Microscopy Co., Ltd) for their relentless support during the critical turning point of my doctoral course. Also, my sincere thanks to the Director General for NIPS Keiji Imoto, Professor Ryuichi Shigemoto (IST Austria), Professor Fukata Masaki (Division of Membrane Physiology, NIPS) and Professor Yugo Fukazawa (Division of Cell Biology and Neuroscience, University of Fukui) for their invaluable help and advice when I needed the most- I would definitely not be here if it were not for them.

Finally, I would like to extend my thanks and appreciation to all the past and present members of the Division of Endocrinology and Metabolism whom I had, and still have, the privilege of working with- they have been very supportive, encouraging and always available to assist where necessary.

REFERENCES

ABMAYR, S. M. & PAVLATH, G. K. 2012. Myoblast fusion: lessons from flies and mice. *Development,* 139**,** 641-56.

ALERS, S., LOFFLER, A. S., WESSELBORG, S. & STORK, B. 2012. Role of AMPK-mTOR-Ulk1/2 in the regulation of autophagy: cross talk, shortcuts, and feedbacks. *Mol Cell Biol,* 32**,** 2-11.

BACH, M., LARANCE, M., JAMES, D. E. & RAMM, G. 2011. The serine/threonine kinase ULK1 is a target of multiple phosphorylation events. *Biochem J,* 440**,** 283-91.

BENTZINGER, C. F., WANG, Y. X. & RUDNICKI, M. A. 2012. Building muscle: molecular regulation of myogenesis. *Cold Spring Harb Perspect Biol,* 4.

BIRK, J. B. & WOJTASZEWSKI, J. F. 2006. Predominant alpha2/beta2/gamma3 AMPK activation during exercise in human skeletal muscle. *J Physiol,* 577**,** 1021-32.

BLAU, H. M., CHIU, C. P. & WEBSTER, C. 1983. Cytoplasmic activation of human nuclear genes in stable heterocaryons. *Cell,* 32**,** 1171-80.

BOLSTER, D. R., CROZIER, S. J., KIMBALL, S. R. & JEFFERSON, L. S. 2002. AMP-activated protein kinase suppresses protein synthesis in rat skeletal muscle through down-regulated mammalian target of rapamycin (mTOR) signaling. *J Biol Chem,* 277**,** 23977-80.

BUNGARD, D., FUERTH, B. J., ZENG, P. Y., FAUBERT, B., MAAS, N. L., VIOLLET, B., CARLING, D., THOMPSON, C. B., JONES, R. G. & BERGER, S. L. 2010. Signaling kinase AMPK activates stress-promoted transcription via histone H2B phosphorylation. *Science,* 329**,** 1201-5.

CHAMBERLAIN, J. S., JAYNES, J. B. & HAUSCHKA, S. D. 1985. Regulation of creatine kinase induction in differentiating mouse myoblasts. *Mol Cell Biol,* 5**,** 484-92.

CHANG, C., SU, H., ZHANG, D., WANG, Y., SHEN, Q., LIU, B., HUANG, R., ZHOU, T., PENG, C., WONG, C. C., SHEN, H. M., LIPPINCOTT-SCHWARTZ, J. & LIU, W. 2015. AMPK-Dependent Phosphorylation of GAPDH Triggers Sirt1 Activation and Is Necessary for Autophagy upon Glucose Starvation. *Mol Cell,* 60**,** 930-40.

CHENG, C. S., EL-ABD, Y., BUI, K., HYUN, Y. E., HUGHES, R. H., KRAUS, W. E. & TRUSKEY, G. A. 2014. Conditions that promote primary human skeletal myoblast culture and muscle differentiation in vitro. *Am J Physiol Cell Physiol,* 306**,** C385-95.

CHEUNG, P. C., SALT, I. P., DAVIES, S. P., HARDIE, D. G. & CARLING, D. 2000. Characterization of AMP-activated protein kinase gamma-subunit isoforms and their role in AMP binding. *Biochem J,* 346 Pt 3**,** 659-69.

EGAN, B. & ZIERATH, J. R. 2013. Exercise metabolism and the molecular regulation of skeletal muscle adaptation. *Cell Metab,* 17**,** 162-84.

EGAN, D. F., SHACKELFORD, D. B., MIHAYLOVA, M. M., GELINO, S., KOHNZ, R. A., MAIR, W., VASQUEZ, D. S., JOSHI, A., GWINN, D. M., TAYLOR, R., ASARA, J. M., FITZPATRICK, J., DILLIN, A., VIOLLET, B., KUNDU, M., HANSEN, M. & SHAW, R. J. 2011. Phosphorylation of ULK1 (hATG1) by AMP-activated protein kinase connects energy sensing to mitophagy. *Science,* 331**,** 456-61.

FU, X., ZHAO, J. X., LIANG, J., ZHU, M. J., FORETZ, M., VIOLLET, B. & DU, M. 2013a. AMP-activated protein kinase mediates myogenin expression and myogenesis via histone deacetylase 5. *Am J Physiol Cell Physiol,* 305**,** C887-95.

FU, X., ZHAO, J. X., ZHU, M. J., FORETZ, M., VIOLLET, B., DODSON, M. V. & DU, M. 2013b. AMP-activated protein kinase alpha1 but not alpha2 catalytic subunit potentiates myogenin expression and myogenesis. *Mol Cell Biol,* 33**,** 4517-25.

FU, X., ZHU, M., ZHANG, S., FORETZ, M., VIOLLET, B. & DU, M. 2016. Obesity Impairs Skeletal Muscle Regeneration Through Inhibition of AMPK. *Diabetes,* 65**,** 188-200.

FUJII, N., SEIFERT, M. M., KANE, E. M., PETER, L. E., HO, R. C., WINSTEAD, S., HIRSHMAN, M. F. & GOODYEAR, L. J. 2007. Role of AMP-activated protein kinase in exercise capacity, whole body glucose homeostasis, and glucose transport in skeletal muscle -insight from analysis of a transgenic mouse model. *Diabetes Res Clin Pract,* 77 Suppl 1**,** S92-8.

FULCO, M. & SARTORELLI, V. 2008. Comparing and contrasting the roles of AMPK and SIRT1 in metabolic tissues. *Cell Cycle,* 7**,** 3669-79.

FULLERTON, M. D., GALIC, S., MARCINKO, K., SIKKEMA, S., PULINILKUNNIL, T., CHEN, Z. P., O'NEILL, H. M., FORD, R. J., PALANIVEL, R., O'BRIEN, M., HARDIE, D. G., MACAULAY, S. L., SCHERTZER, J. D., DYCK, J. R., VAN DENDEREN, B. J., KEMP, B. E. & STEINBERG, G. R. 2013. Single phosphorylation sites in Acc1 and Acc2 regulate lipid homeostasis and the insulin-sensitizing effects of metformin. *Nat Med,* 19**,** 1649-54.

GAVET, O. & PINES, J. 2010. Progressive activation of CyclinB1-Cdk1 coordinates entry to mitosis. *Dev Cell,* 18**,** 533-43.

GOWANS, G. J., HAWLEY, S. A., ROSS, F. A. & HARDIE, D. G. 2013. AMP is a true physiological regulator of AMP-activated protein kinase by both allosteric activation and enhancing net phosphorylation. *Cell Metab,* 18**,** 556-66.

HARDIE, D. G. 2011. AMP-activated protein kinase: an energy sensor that regulates all aspects of cell function. *Genes Dev,* 25**,** 1895-908.

HARDIE, D. G., ROSS, F. A. & HAWLEY, S. A. 2012. AMPK: a nutrient and energy sensor that maintains energy homeostasis. *Nat Rev Mol Cell Biol,* 13**,** 251-62.

HAWLEY, J. A., HARGREAVES, M. & ZIERATH, J. R. 2006. Signalling mechanisms in skeletal muscle: role in substrate selection and muscle adaptation. *Essays Biochem,* 42**,** 1-12.

HINDI, S. M., TAJRISHI, M. M. & KUMAR, A. 2013. Signaling mechanisms in mammalian myoblast fusion. *Sci Signal,* 6**,** re2.

IRRCHER, I., LJUBICIC, V., KIRWAN, A. F. & HOOD, D. A. 2008. AMP-activated protein kinase-regulated activation of the PGC-1alpha promoter in skeletal muscle cells. *PLoS One,* 3**,** e3614.

JOHNSON, J. E., WOLD, B. J. & HAUSCHKA, S. D. 1989. Muscle creatine kinase sequence elements regulating skeletal and cardiac muscle expression in transgenic mice. *Mol Cell Biol,* 9**,** 3393-9.

KIM, J., KUNDU, M., VIOLLET, B. & GUAN, K. L. 2011. AMPK and mTOR regulate autophagy through direct phosphorylation of Ulk1. *Nat Cell Biol,* 13**,** 132-41.

KNIGHT, J. D. & KOTHARY, R. 2011. The myogenic kinome: protein kinases critical to mammalian skeletal myogenesis. *Skelet Muscle,* 1**,** 29.

LANTIER, L., FENTZ, J., MOUNIER, R., LECLERC, J., TREEBAK, J. T., PEHMOLLER, C., SANZ, N., SAKAKIBARA, I., SAINT-AMAND, E., RIMBAUD, S., MAIRE, P., MARETTE, A., VENTURA-CLAPIER, R., FERRY, A., WOJTASZEWSKI, J. F., FORETZ, M. & VIOLLET, B. 2014. AMPK controls exercise endurance, mitochondrial oxidative capacity, and skeletal muscle integrity. *FASEB J,* 28**,** 3211-24.

LEE, Y. K., LEE, W. S., KIM, G. S. & PARK, O. J. 2010a. Anthocyanins are novel AMPKalpha1 stimulators that suppress tumor growth by inhibiting mTOR phosphorylation. *Oncol Rep,* 24**,** 1471-7.

LEE, Y. K., PARK, S. Y., KIM, Y. M., KIM, D. C., LEE, W. S., SURH, Y. J. & PARK, O. J. 2010b. Suppression of mTOR via Akt-dependent and -independent mechanisms in selenium-treated colon cancer cells: involvement of AMPKalpha1. *Carcinogenesis,* 31**,** 1092-9.

MAHLAPUU, M., JOHANSSON, C., LINDGREN, K., HJALM, G., BARNES, B. R., KROOK, A., ZIERATH, J. R., ANDERSSON, L. & MARKLUND, S. 2004. Expression profiling of the gamma-subunit isoforms of AMP-activated protein kinase suggests a major role for gamma3 in white skeletal muscle. *Am J Physiol Endocrinol Metab,* 286**,** E194-200.

MCCLOY, R. A., ROGERS, S., CALDON, C. E., LORCA, T., CASTRO, A. & BURGESS, A. 2014. Partial inhibition of Cdk1 in G 2 phase overrides the SAC and decouples mitotic events. *Cell Cycle,* 13**,** 1400-12.

MCGEE, S. L., FAIRLIE, E., GARNHAM, A. P. & HARGREAVES, M. 2009. Exercise-induced histone modifications in human skeletal muscle. *J Physiol,* 587**,** 5951-8.

MCGEE, S. L., HOWLETT, K. F., STARKIE, R. L., CAMERON-SMITH, D., KEMP, B. E. & HARGREAVES, M. 2003. Exercise increases nuclear AMPK alpha2 in human skeletal muscle. *Diabetes,* 52**,** 926-8.

MERLEN, G., GENTRIC, G., CELTON-MORIZUR, S., FORETZ, M., GUIDOTTI, J. E., FAUVEAU, V., LECLERC, J., VIOLLET, B. & DESDOUETS, C. 2014. AMPKalpha1 controls hepatocyte proliferation independently of energy balance by regulating Cyclin A2 expression. *J Hepatol,* 60**,** 152-9.

MIHAYLOVA, M. M. & SHAW, R. J. 2011. The AMPK signalling pathway coordinates cell growth, autophagy and metabolism. *Nat Cell Biol,* 13**,** 1016-23.

MINOKOSHI, Y., KIM, Y. B., PERONI, O. D., FRYER, L. G., MULLER, C., CARLING, D. & KAHN, B. B. 2002. Leptin stimulates fatty-acid oxidation by activating AMP-activated protein kinase. *Nature,* 415**,** 339-43.

MOUNIER, R., LANTIER, L., LECLERC, J., SOTIROPOULOS, A., PENDE, M., DAEGELEN, D., SAKAMOTO, K., FORETZ, M. & VIOLLET, B. 2009. Important role for AMPKalpha1 in limiting skeletal muscle cell hypertrophy. *Faseb j,* 23**,** 2264-73.

MOUNIER, R., THERET, M., LANTIER, L., FORETZ, M. & VIOLLET, B. 2015. Expanding roles for AMPK in skeletal muscle plasticity. *Trends Endocrinol Metab,* 26**,** 275-86.

MU, J., BROZINICK, J. T., JR., VALLADARES, O., BUCAN, M. & BIRNBAUM, M. J. 2001. A role for AMP-activated protein kinase in contraction- and hypoxia-regulated glucose transport in skeletal muscle. *Mol Cell,* 7**,** 1085-94.

NADER, G. A., HORNBERGER, T. A. & ESSER, K. A. 2002. Translational control: implications for skeletal muscle hypertrophy. *Clin Orthop Relat Res***,** S178-87.

REZNICK, R. M. & SHULMAN, G. I. 2006. The role of AMP-activated protein kinase in mitochondrial biogenesis. *J Physiol,* 574**,** 33-9.

ROHAS, L. M., ST-PIERRE, J., ULDRY, M., JAGER, S., HANDSCHIN, C. & SPIEGELMAN, B. M. 2007. A fundamental system of cellular energy homeostasis regulated by PGC-1alpha. *Proc Natl Acad Sci U S A,* 104**,** 7933-8.

ROSS, F. A., MACKINTOSH, C. & HARDIE, D. G. 2016. AMP-activated protein kinase: a cellular energy sensor that comes in twelve flavours. *Febs j*.

SALT, I., CELLER, J. W., HAWLEY, S. A., PRESCOTT, A., WOODS, A., CARLING, D. & HARDIE, D. G. 1998. AMP-activated protein kinase: greater AMP dependence, and preferential nuclear localization, of complexes containing the alpha2 isoform. *Biochem J,* 334 (Pt 1)**,** 177-87.

SPANDIDOS, A., WANG, X., WANG, H., DRAGNEV, S., THURBER, T. & SEED, B. 2008. A comprehensive collection of experimentally validated primers for Polymerase Chain Reaction quantitation of murine transcript abundance. *BMC Genomics,* 9**,** 633.

SPANDIDOS, A., WANG, X., WANG, H. & SEED, B. 2010. PrimerBank: a resource of human and mouse PCR primer pairs for gene expression detection and quantification. *Nucleic Acids Res,* 38**,** D792-9.

SRIWIJITKAMOL, A., COLETTA, D. K., WAJCBERG, E., BALBONTIN, G. B., REYNA, S. M., BARRIENTES, J., EAGAN, P. A., JENKINSON, C. P., CERSOSIMO, E., DEFRONZO, R. A., SAKAMOTO, K. & MUSI, N. 2007. Effect of acute exercise on AMPK signaling in

skeletal muscle of subjects with type 2 diabetes: a time-course and dose-response study. *Diabetes,* 56**,** 836-48.

STAPLETON, D., MITCHELHILL, K. I., GAO, G., WIDMER, J., MICHELL, B. J., TEH, T., HOUSE, C. M., FERNANDEZ, C. S., COX, T., WITTERS, L. A. & KEMP, B. E. 1996. Mammalian AMP-activated protein kinase subfamily. *J Biol Chem,* 271**,** 611-4.

SUZUKI, A., OKAMOTO, S., LEE, S., SAITO, K., SHIUCHI, T. & MINOKOSHI, Y. 2007. Leptin stimulates fatty acid oxidation and peroxisome proliferator-activated receptor alpha gene expression in mouse C2C12 myoblasts by changing the subcellular localization of the alpha2 form of AMP-activated protein kinase. *Mol Cell Biol,* 27**,** 4317-27.

THOMSON, D. M. & GORDON, S. E. 2005. Diminished overload-induced hypertrophy in aged fast-twitch skeletal muscle is associated with AMPK hyperphosphorylation. *J Appl Physiol (1985),* 98**,** 557-64.

THOMSON, D. M., HERWAY, S. T., FILLMORE, N., KIM, H., BROWN, J. D., BARROW, J. R. & WINDER, W. W. 2008. AMP-activated protein kinase phosphorylates transcription factors of the CREB family. *J Appl Physiol (1985),* 104**,** 429-38.

THORNTON, C., SNOWDEN, M. A. & CARLING, D. 1998. Identification of a novel AMP-activated protein kinase beta subunit isoform that is highly expressed in skeletal muscle. *J Biol Chem,* 273**,** 12443-50.

TOWLER, M. C. & HARDIE, D. G. 2007. AMP-activated protein kinase in metabolic control and insulin signaling. *Circ Res,* 100**,** 328-41.

VAVVAS, D., APAZIDIS, A., SAHA, A. K., GAMBLE, J., PATEL, A., KEMP, B. E., WITTERS, L. A. & RUDERMAN, N. B. 1997. Contraction-induced changes in acetyl-CoA carboxylase and 5'-AMP-activated kinase in skeletal muscle. *J Biol Chem,* 272**,** 13255-61.

VENTURA-CLAPIER, R., GARNIER, A. & VEKSLER, V. 2008. Transcriptional control of mitochondrial biogenesis: the central role of PGC-1alpha. *Cardiovasc Res,* 79**,** 208-17.

VIOLLET, B., ATHEA, Y., MOUNIER, R., GUIGAS, B., ZARRINPASHNEH, E., HORMAN, S., LANTIER, L., HEBRARD, S., DEVIN-LECLERC, J., BEAULOYE, C., FORETZ, M., ANDREELLI, F., VENTURA-CLAPIER, R. & BERTRAND, L. 2009. AMPK: Lessons from transgenic and knockout animals. *Front Biosci (Landmark Ed),* 14**,** 19-44.

VISSING, K., MCGEE, S. L., ROEPSTORFF, C., SCHJERLING, P., HARGREAVES, M. & KIENS, B. 2008. Effect of sex differences on human MEF2 regulation during endurance exercise. *Am J Physiol Endocrinol Metab,* 294**,** E408-15.

WANG, X. & SEED, B. 2003. A PCR primer bank for quantitative gene expression analysis. *Nucleic Acids Res,* 31**,** e154.

WINDER, W. W., WILSON, H. A., HARDIE, D. G., RASMUSSEN, B. B., HUTBER, C. A., CALL, G. B., CLAYTON, R. D., CONLEY, L. M., YOON, S. & ZHOU, B. 1997. Phosphorylation of rat muscle acetyl-CoA carboxylase by AMP-activated protein kinase and protein kinase A. *J Appl Physiol (1985),* 82**,** 219-25.

WOJTASZEWSKI, J. F., BIRK, J. B., FROSIG, C., HOLTEN, M., PILEGAARD, H. & DELA, F. 2005. 5'AMP activated protein kinase expression in human skeletal muscle: effects of strength training and type 2 diabetes. *J Physiol,* 564**,** 563-73.

YAFFE, D. & SAXEL, O. 1977. Serial passaging and differentiation of myogenic cells isolated from dystrophic mouse muscle. *Nature,* 270**,** 725-7.

ZONG, H., REN, J. M., YOUNG, L. H., PYPAERT, M., MU, J., BIRNBAUM, M. J. & SHULMAN, G. I. 2002. AMP kinase is required for mitochondrial biogenesis in skeletal muscle in response to chronic energy deprivation. *Proc Natl Acad Sci U S A,* 99**,** 15983-7.

Table I: Primer sequences for Real-Time quantitative PCR and standard PCR analyses

Target	Sequence ($5^1 \rightarrow 3^1$)
AMPKα1	F: AGAGGGCCGCAATAAAAGAT R: TGTTGTACAGGCAGCTGAGG
AMPKα2	F: ACAGCGCCATGCATATTCCTC R: ATGTCACACGCTTTGCTCTG
MyoD1*	F: CCACTCCGGGACATAGACTTG R: AAAAGCGCAGGTCTGGTGAG
Myogenin	F: GGTGTGTAAGAGGAAGTCTGTG R: TAGGCGCTCAATGTACTGGAT
Muscle Creatine Kinase	F: CTGACCCCTGACCTCTACAAT R: CATGGCGGTCCTGGATGAT
Ppargc1a*	F: TATGGAGTGACATAGAGTGTGCT R: CCACTTCAATCCACCCAGAAAG
TFAM	F: CCAAAAAGACCTCGTTCAGC R: CTTCAGCCATCTGCTCTTCC
NRF-2	F: CCGCTACACCGACTAGGATT R: ACCTTCATCACCAACCCAAG
TFB2M	F: TCCACATTTGGAGCCCTTAC R: ACACCTGCTGACCAAGGAAC
36B4	F: GGCCCTGCACTCTCGCTTTC R: TGCCAGGACGCGCTTGT
GAPDH (PCR)	F: AACTTTGGCATTGTGGAAGG R: ACACATTGGGGGTAGGAACA
FLAG (PCR)	F: GATTACAAGGACGATGACGACAAG R: ATTTAGTACAGGCAGCTGAGGA

* Primer sequences were obtained from Harvard PrimerBank [Wang and Seed (2003); Spandidos et al. (2008); Spandidos et al. (2010)].

Table II: List of Primary Antibodies used for Western Blotting (WB) and Immunofluorescence (IF) Analyses

Antigen	Catalogue Number	Product Company	Dilution Factor
AMPKα	2532	Cell Signaling Technology, Danvers, MA	1:1000 (WB)
Phospho-AMPKα (Thr172)	2535	Cell Signaling Technology, Danvers, MA	1:2000 (WB)
Acetyl-CoA Carboxylase	3676	Cell Signaling Technology, Danvers, MA	1:1000 (WB)
Phospho-Acetyl-CoA Carboxylase (Ser79)	3661	Cell Signaling Technology, Danvers, MA	1:1000 (WB)
B- Actin	4967	Cell Signaling Technology, Danvers, MA	1:1000 (WB)
α-Tubulin	2144	Cell Signaling Technology, Danvers, MA	1:1000 (WB)
Phospho-ULK1 (Ser555)	5869	Cell Signaling Technology, Danvers, MA	1:1000 (WB)
ATG1/ULK1	A7481	Sigma-Aldrich, St. Louis, MO	1:1000 (WB)
FLAG	F7425	Sigma-Aldrich, St. Louis, MO	1:750 (IF)
AMPKα1	Ab32047	Abcam, Cambridge, UK	1:1000
AMPKα2	Ab3760	Abcam, Cambridge, UK	1:1000 (WB) 1:750 (IF)
AMPKα1		In-house produced	
AMPKα2		In-house produced	

FIGURE LEGENDS

Figure 1 | Effect of AMPKα isoforms on C2C12 myoblast proliferation

(A to D) FACS analysis of control, shPanAMPK, shAMPKα1 and shAMPKα2 myoblasts after infection with their respective lentivirus vectors. Myoblast population from the individual cell lines was selected from a backscatter (BSC) vs forward scatter (FSC) density plot (left panel), after which the appropriate gating was performed on the selected population by generating a bivariate histogram (middle panel). Bottom right quadrant (Q4) of the histogram represents EGFP-positive cells that were isolated and used for subsequent cultures. Right panel shows representative images of the EGFP-sorted myoblasts. Scale bar = 200 μm. **(E)** Representative phase-contrast images of control, shPanAMPK, shAMPKα1 and shAMPKα2 myoblasts taken at different time points (24hr, 48hr and 72hr). Scale bar = 100 μm. **(F)** Growth curve assay of control, shPanAMPK, shAMPKα1 and shAMPKα2 myoblasts that were cultured for 72hr, during which cells were collected and counted at 24hr intervals. Data are shown as means ± s.e.m. (n=3) $^{*}P < 0.05$ versus control, $^{\dagger}P < 0.05$ versus shAMPKα2, $^{\ddagger}P < 0.05$ versus shPanAMPK.

Figure 2 | Changes in α1- and α2-AMPK mRNA and protein expressions during myogenic differentiation

(A, B) RT-qPCR analysis of α1- and α2- AMPK mRNA abundance in 24hr myoblasts, 24hr-, 72hr- and 6days myotubes of control, shPanAMPK, shAMPKα1 and shAMPKα2 C2C12 cell lines. Data are shown as means ± s.e.m. (n=3) $^{*}P < 0.05$ versus control, $^{\dagger}P < 0.05$ versus corresponding values to 24hr myoblasts. **(C)** Immunoblot analysis of AMPKα1,

AMPKα2, total AMPKα and β-actin contents in 24hr-, 72hr- and 6days myotubes of control, shPanAMPK, shAMPKα1 and shAMPKα2 C2C12 cell lines.

Figure 3 | Phenotypic effects of AMPKα on myogenic differentiation

(A) Representative images of EGFP-expressing control, shPanAMPK, shAMPKα1 and shAMPKα2 myotubes captured under fluorescence microscope, 6 days after inducing differentiation. Scale bar = 200 μm. **(B)** Representative image of how the diameters for individual myotubes were measured in one field. Three short-axis measurements were taken along the length of a selected myotube and the average was calculated. *Insert diagram* depicts the selection criteria of myotubes for measuring of individual diameters. Selected myotubes should be of a length that is more than that of three myoblasts. Also, they should contain more than three nuclei in a single alignment. **(C)** Frequency histogram showing the distribution of myotube size for control, shPanAMPK, shAMPKα1 and shAMPKα2 myotubes 6 days after inducing myogenic differentiation. Data are shown as means ± s.e.m. (n=3). *Insert images* are representative (magnified) images of control, shPanAMPK, shAMPKα1 and shAMPKα2 myotubes, depicting the differences in myotube diameter size among the cell lines after 6 days of differentiation. **(D)** Cumulative frequency curve showing the number of cells versus cell diameter.

Figure 4 | Expression of myogenic markers during differentiation of control, shPanAMPK, shAMPKα1 and shAMPKα2 cell lines

(A) Illustration depicting skeletal muscle differentiation process in C2C12 cells. MyoD, Myogenin and MCK are expressed during the early, middle and late stage of myogenic

differentiation respectively. **(B to D)** RT-qPCR analysis of MyoD1, myogenin and muscle creatine kinase mRNA abundance in 24hr myoblasts, 24hr-, 72hr- and 6days myotubes of control C2C12 cell line. $^{*}P < 0.05$ versus 24hr myoblasts, $^{\dagger}P < 0.05$ versus corresponding values to 72hr myotubes. **(E to G)** RT-qPCR analysis of MyoD1, myogenin and muscle creatine kinase mRNA abundance in control, shPanAMPK, shAMPKα1 and shAMPKα2 C2C12 cell lines for 24hr myotubes, 72hr myotubes and 6days myotubes respectively. $^{*}P < 0.05$ versus control. All data are shown as means ± s.e.m. (n=3).

Figure 5 | Effects of AMPKα2 knockdown on mitochondrial biogenesis

(A to D) RT-qPCR analysis of PGC-1α, TFB2M, Tfam and NRF-2 mRNA abundance in control, shPanAMPK, shAMPKα1 and shAMPKα2 myotubes, after 6 days of differentiation. Data are shown as means ± s.e.m. (n=3) $^{*}P < 0.05$ versus control. **(E)** Tetramethylrhodamine methyl ester (TMRM) staining of control, shPanAMPK, shAMPKα1 and shAMPKα2 myotubes, after 6 days of differentiation. Scale bar = 200 μm. **(F)** Graphs show quantification of TMRM and EGFP fluorescence intensities from 20 independent regions of interest (ROI) in the respective TMRM and EGFP images. Data are shown as means ± s.e.m. (n=20) $^{*}P < 0.05$ versus control.

Figure 6 | Individual contributions of AMPKα1 and AMPKα2 towards AMPK activity, as well as ACC and ULK1 phosphorylation

(A) Immunoblot analysis of AMPK phosphorylation on Thr172, total AMPKα, AMPKα1, AMPKα2 and β-actin protein contents in control, shPanAMPK, shAMPKα1 and shAMPKα2 myotubes after 6 days of differentiation. **(B and C)** Immunoblot analysis of

AMPKα1- and AMPKα2-specific phosphorylation on Thr172. Cell lysates of control and shPanAMPK myotubes after 6 days of differentiation were immune-precipitated with specific antibody for AMPKα1- and AMPKα2 and subjected to the immunoblot analysis. **(D and E)** Immunoblot analysis of the phosphorylation of ACC on Ser79 and ULK1 on Ser555 in control, shPanAMPK, shAMPKα1 and shAMPKα2 myotubes after 6 days of differentiation.

Figure 7 | Immunofluorescence staining of endogenous AMPKα2 during myogenesis, as well as the effects of AMPK activators on nuclear localisation in WT-AMPKα2- and ΔNLS-AMPKα2- transfected C2C12 myoblasts

(A) Immunofluorescence staining of endogenous AMPKα2 labelled in green (Alexa Fluor 488), as well as nuclear staining with DAPI, in 24hr myoblasts, 24hr-, 72hr- and 6days myotubes of C2C12 intact cell line. White arrows indicate co-localisation between AMPKα2 and DAPI fluorescence. Scale bar = 200 μm. **(B)** Schematic diagram depicting amino acid sequences of putative nuclear localisation signal (NLS) present in the α2 subunit of AMPK, but not in α1. Site-directed mutagenesis was performed on the NLS sequence (K224A) to generate ΔNLS-AMPKα2. **(C)** C2C12 myoblasts transiently expressing FLAG-α2 (WT and ΔNLS) were incubated in the absence (control) or presence of AICAR and low glucose plus 2DG (LG-2DG) for 1hr and then subjected to immunofluorescence staining with anti-FLAG and DAPI. Scale bar = 200 μm. **(D and E)** The numbers of cells, in which FLAG-α2 was detected in the cytoplasm or in both the cytoplasm and nucleus after treatment with AICAR and LG-2DG. A total of 500 transfected cells from six independent fields were counted for each group. Data are

shown as means ± s.e.m. (n=6) *$P < 0.05$ versus cytoplasm, †$P < 0.05$ versus (-) AICAR (for Figure D), †$P < 0.05$ versus (-) LG-2DG (for Figure E).

Figure 8 | Effects of overexpressing WT-AMPKα2 and ΔNLS-AMPKα2 on differentiation in control and shAMPKα2 myotubes

(A and B) Representative images of EGFP-expressing control and shAMPKα2 myotubes that were infected with lentiviral vectors expressing WT-AMPKα2 and ΔNLS-AMPKα2, after which they were induced to differentiate for 6 days. Scale bar = 200 μm. **(C and D)** RT-qPCR analysis of α1- and α2-AMPK mRNA abundance in control and shAMPKα2 myotubes expressing WT-AMPKα2 and ΔNLS-AMPKα2, after 6 days of differentiation. Data are shown as means ± s.e.m. (n=5). **(E)** Immunoblot analysis of AMPKα1, AMPKα2 and β-actin in control and shAMPKα2 myotubes expressing WT-AMPKα2 and ΔNLS-AMPKα2, after 6 days of differentiation. **(F)** PCR analysis for FLAG and GAPDH contents in control and shAMPKα2 myotubes expressing WT-AMPKα2 and ΔNLS-AMPKα2, after 6 days of differentiation. **(G and H)** RT-qPCR analysis of muscle creatine kinase and PGC-1α mRNA abundance in control and shAMPKα2 myotubes expressing WT-AMPKα2 and ΔNLS-AMPKα2, after 6 days of differentiation. Data are shown as means ± s.e.m. (n=8) *$P < 0.05$ versus shAMPKα2-Empty.

Figure 9 | Hypothesis model depicting the possible roles of AMPKα1 and AMPKα2 in C2C12 myotubes

AMPKα1 is necessary for the phosphorylation of ACC and ULK1; this, in turn, could mediate the upregulation of fatty acid oxidation and autophagy respectively. On the

other hand, AMPKα2 is essential for the up-regulation of muscle creatine kinase expression but is independent on its nuclear localisation signal. In parallel, while AMPKα2 is also necessary for up-regulating PGC-1α expression and possibly mitochondrial biogenesis, this effect relies upon its nuclear localisation signal. Those effects of AMPKα2 may be associated with the width of C2C12 myotubes.

Figure 1

A Control

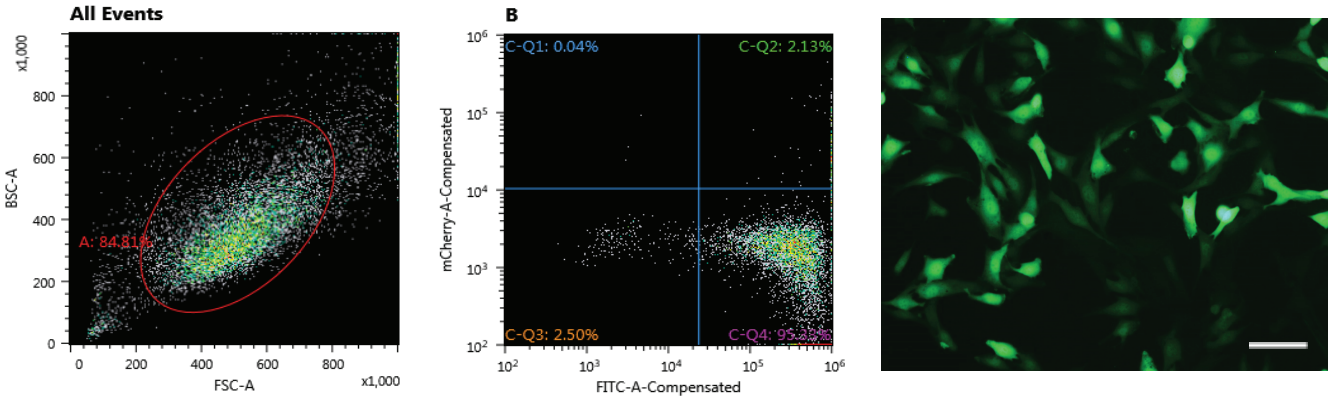

B shPanAMPK

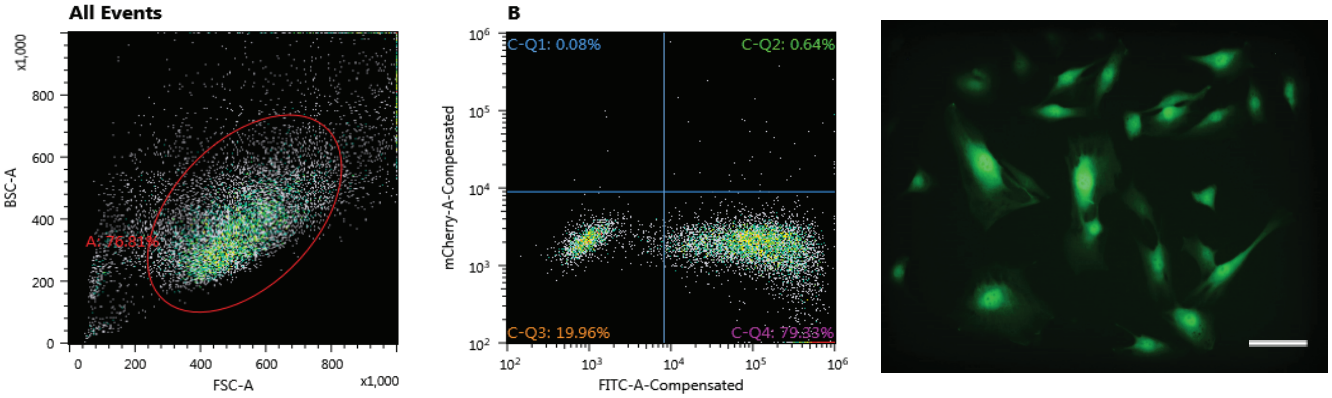

C shAMPKα1

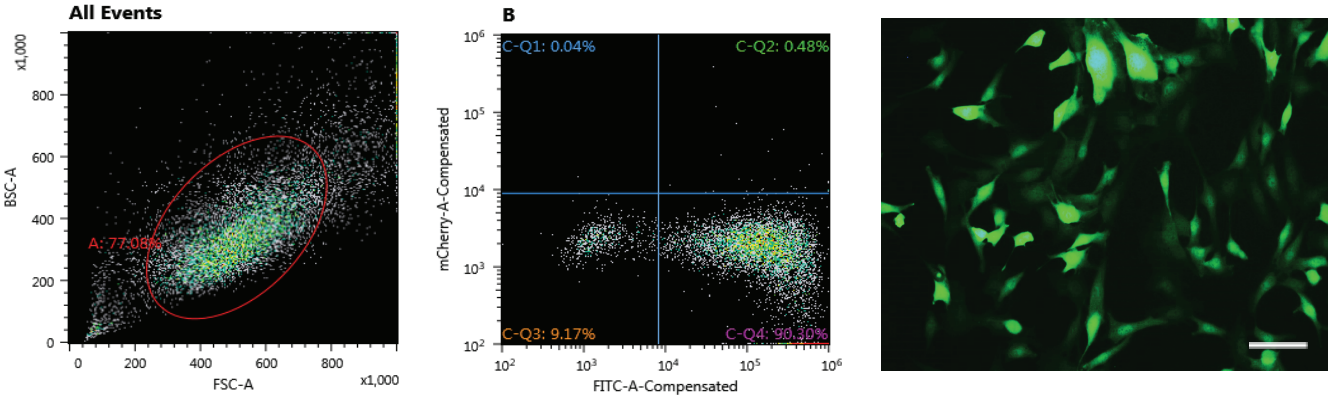

D shAMPKα2

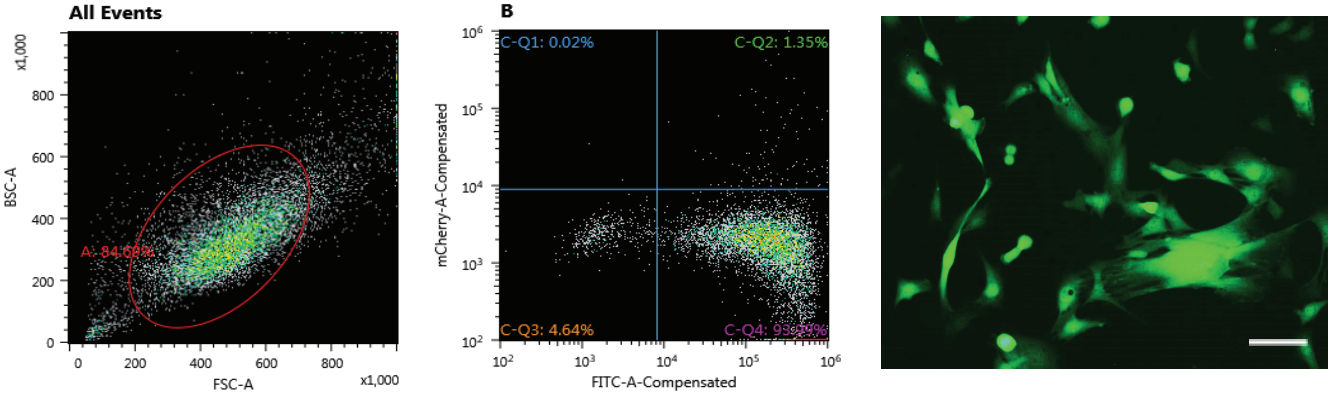

Figure 1 (continued)

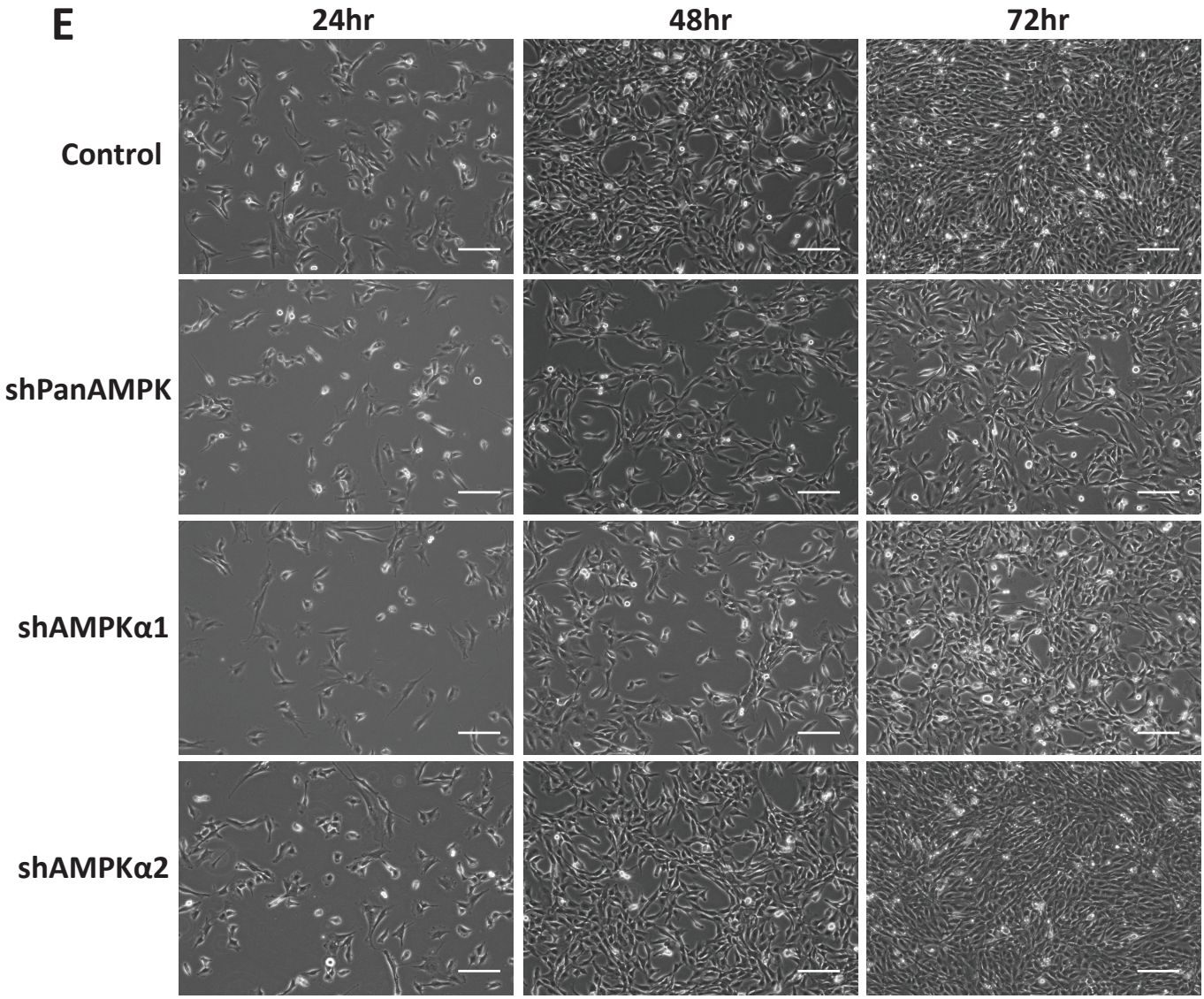

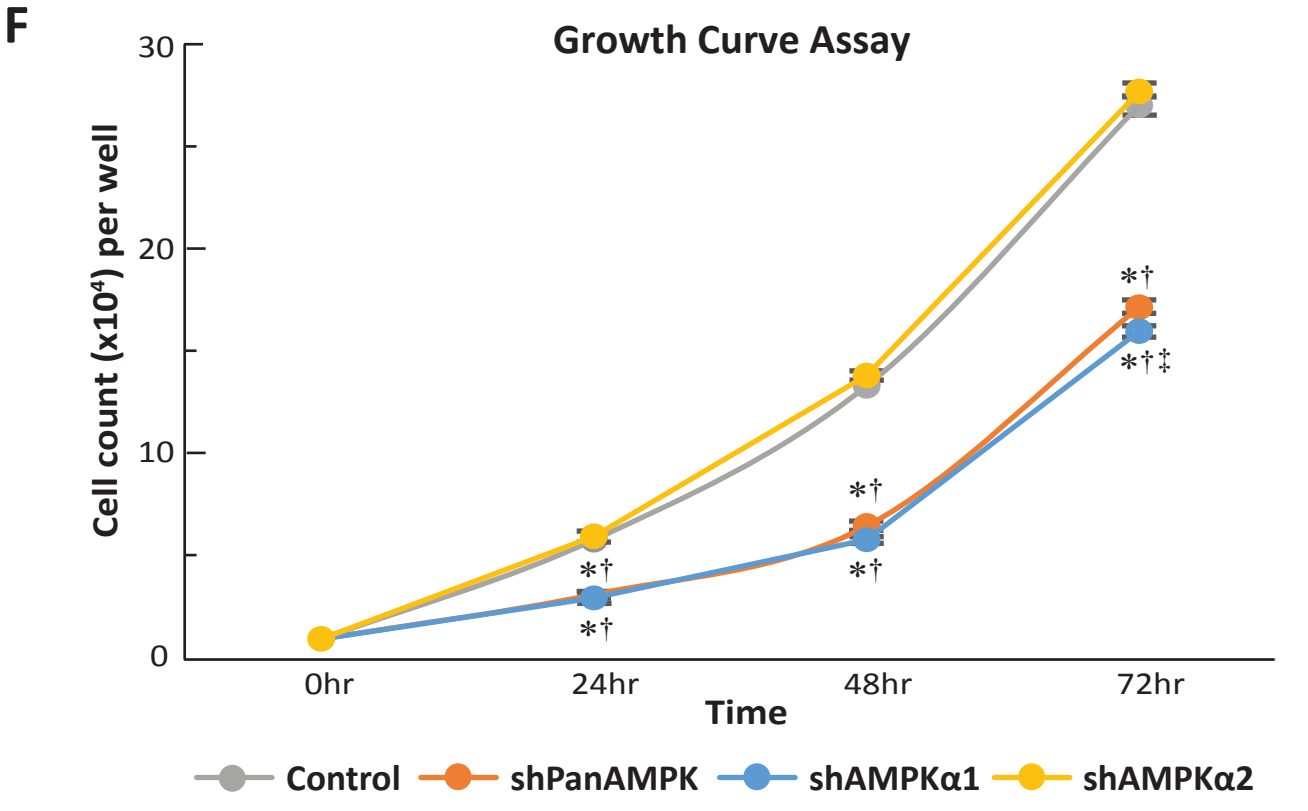

Figure 2

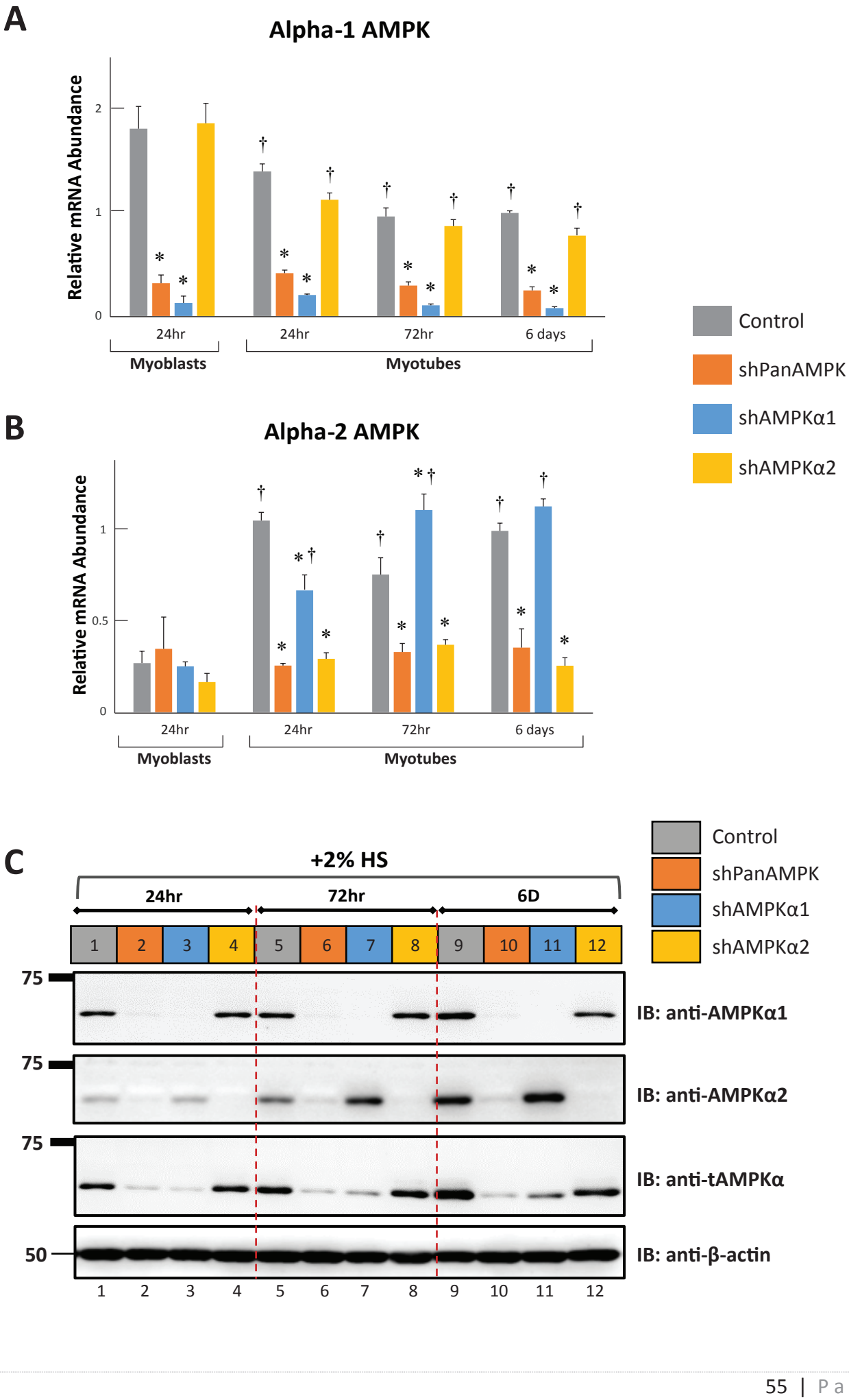
A
Alpha-1 AMPK
Relative mRNA Abundance
2
1
0
24hr
24hr
72hr
6 days
Myoblasts
Myotubes
B
Alpha-2 AMPK
Relative mRNA Abundance
1
0.5
0
24hr
24hr
72hr
6 days
Myoblasts
Myotubes
Control
shPanAMPK
shAMPKα1
shAMPKα2
C
+2% HS
24hr
72hr
6D
1 2 3 4 5 6 7 8 9 10 11 12
75
IB: anti-AMPKα1
75
IB: anti-AMPKα2
75
IB: anti-tAMPKα
50
IB: anti-β-actin
1 2 3 4 5 6 7 8 9 10 11 12
Control
shPanAMPK
shAMPKα1
shAMPKα2

Figure 3

A

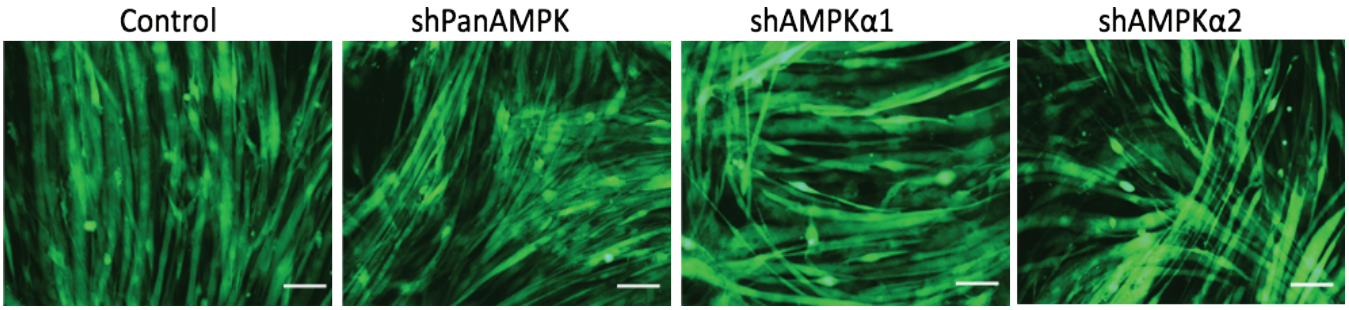

B

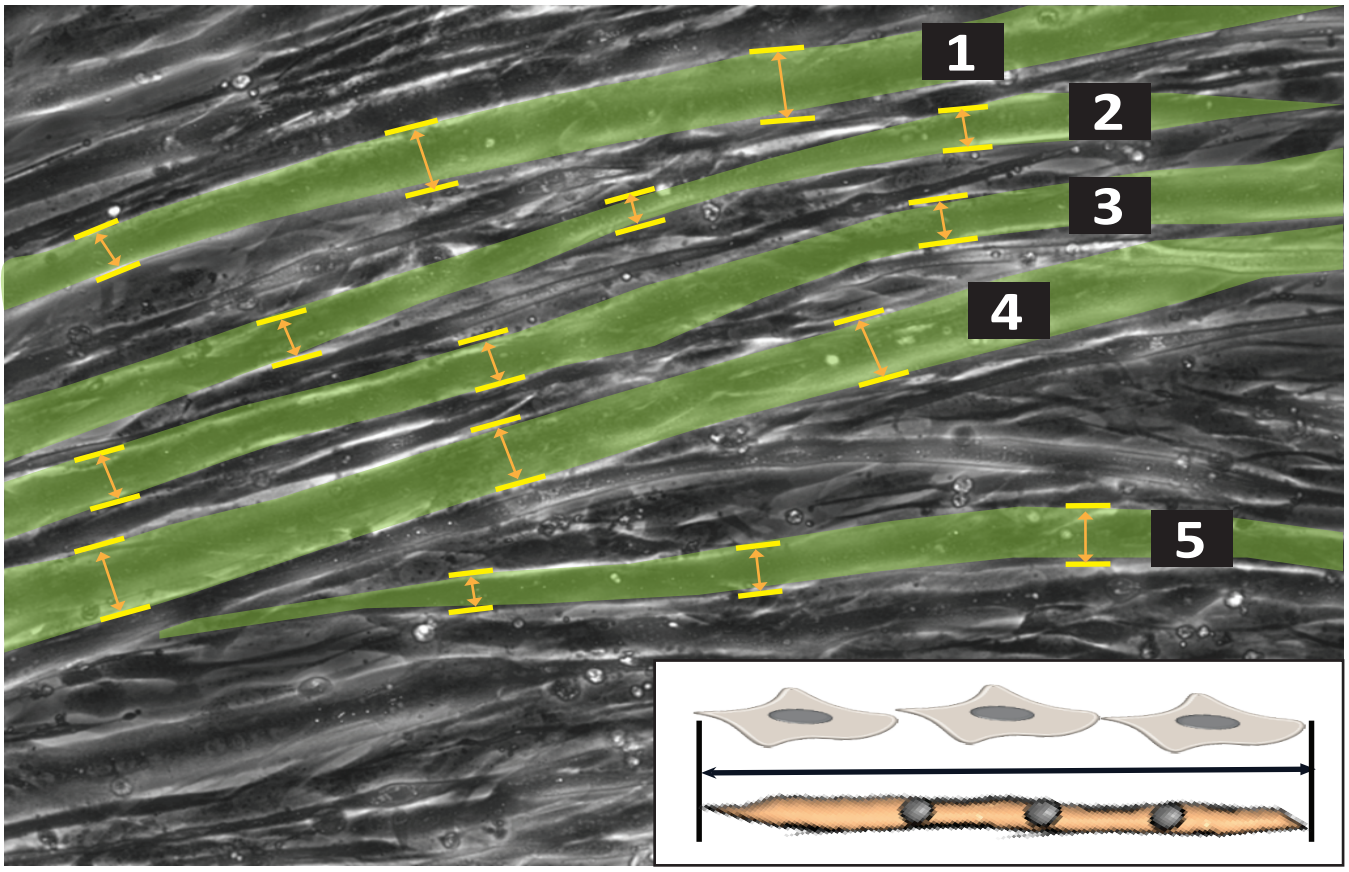

Figure 3 (continued)

C

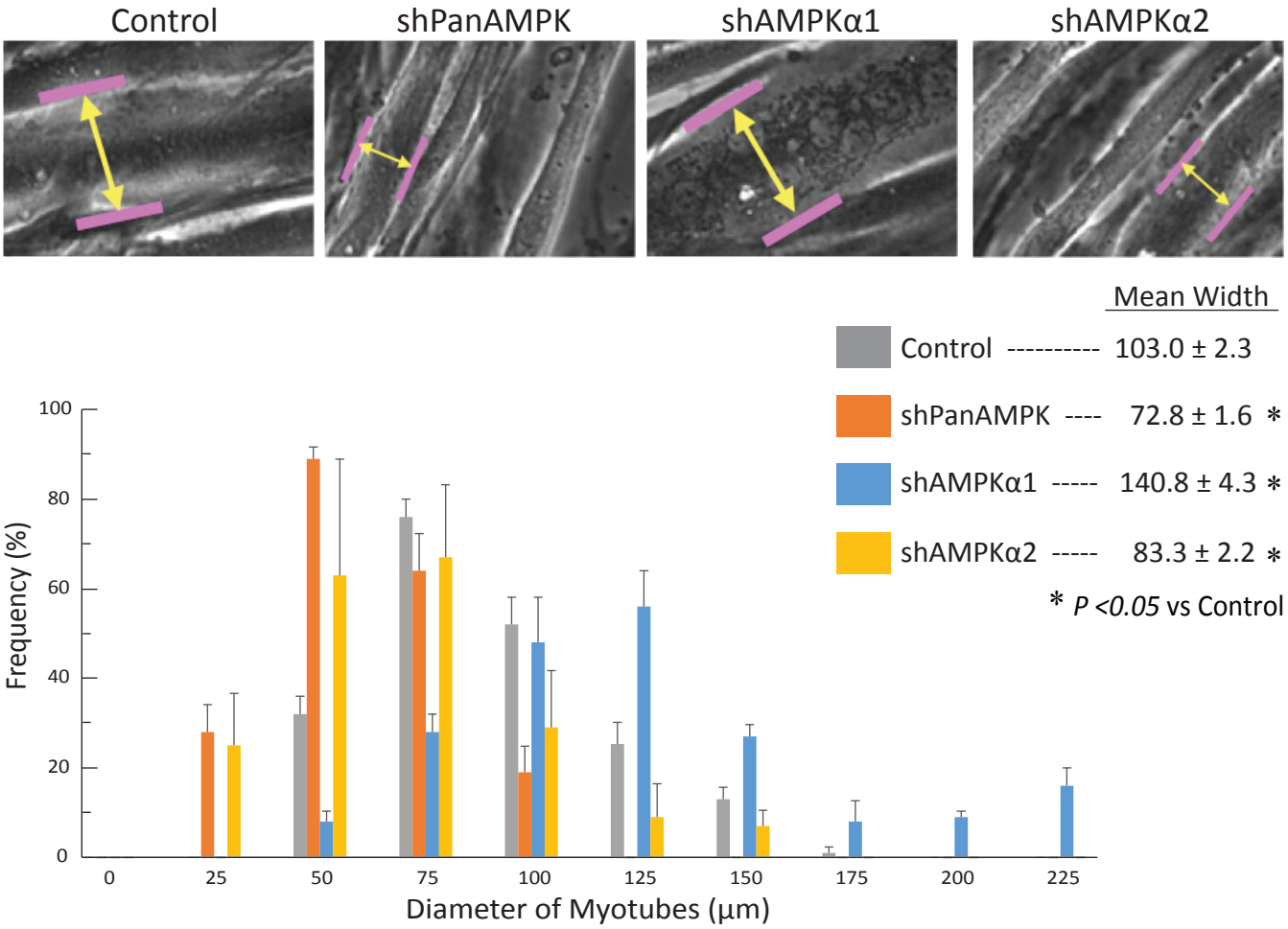

D

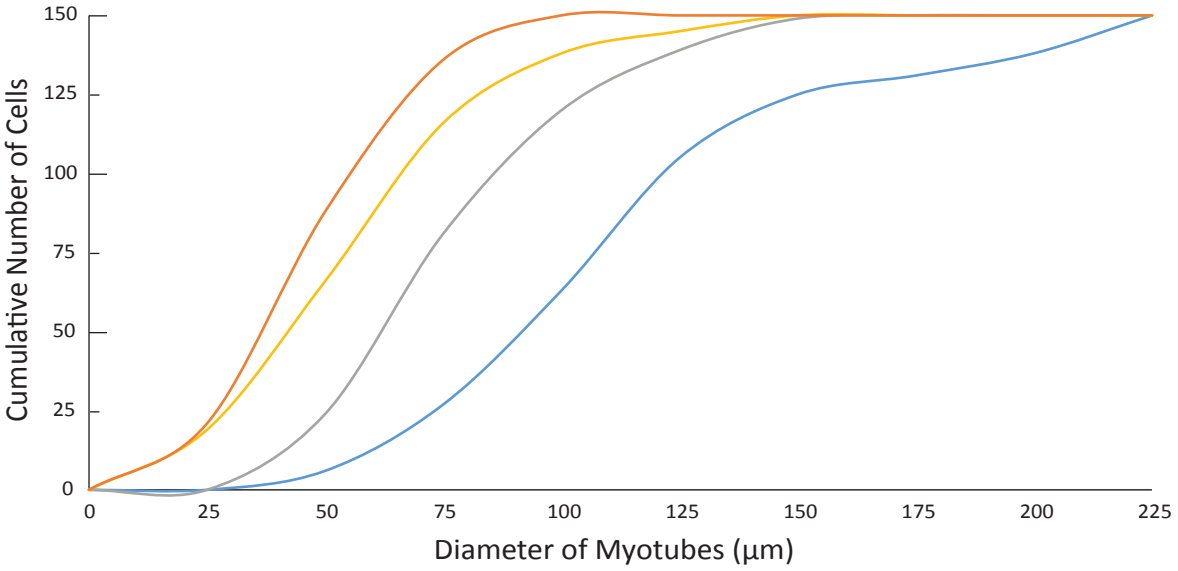

Figure 4

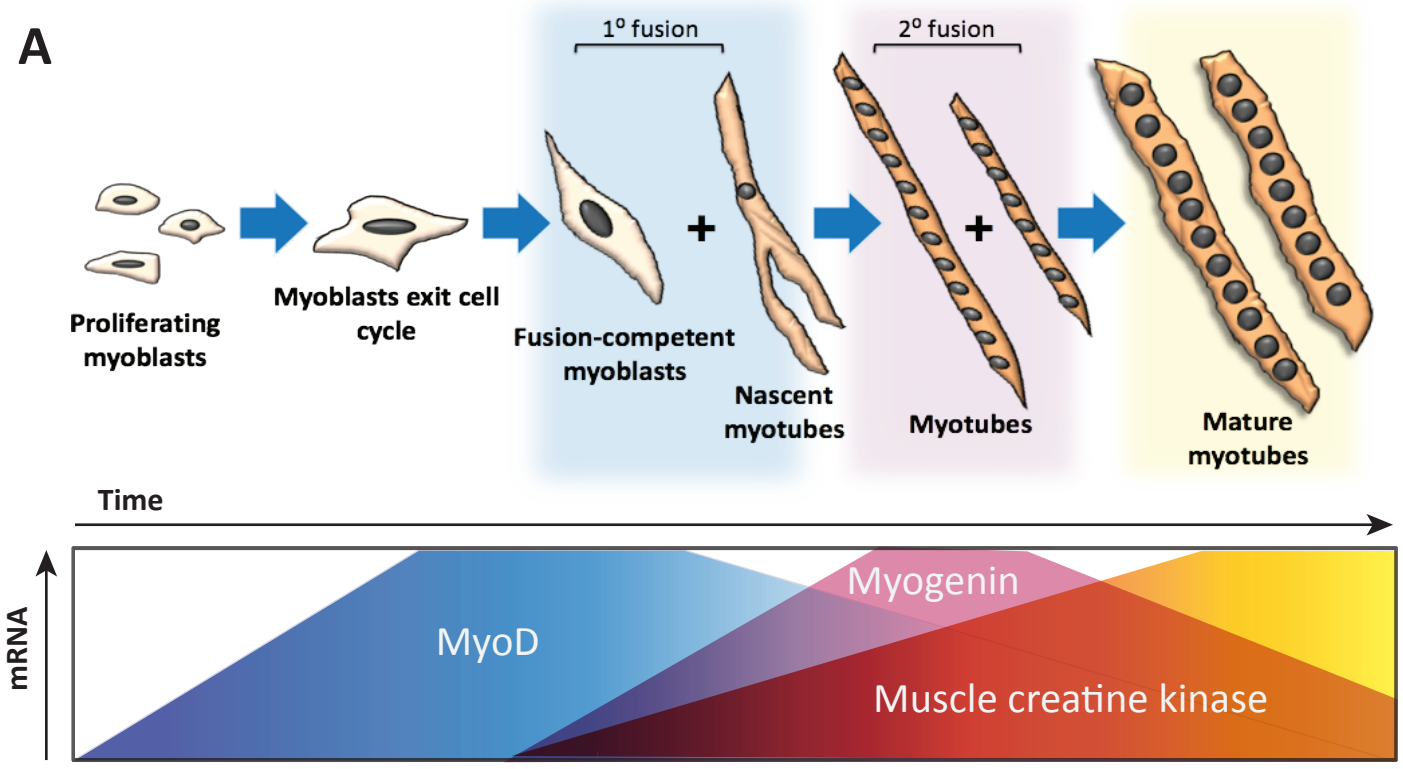
A
1° fusion
2° fusion
Proliferating myoblasts
Myoblasts exit cell cycle
Fusion-competent myoblasts
Nascent myotubes
Myotubes
Mature myotubes
Time
mRNA
MyoD
Myogenin
Muscle creatine kinase

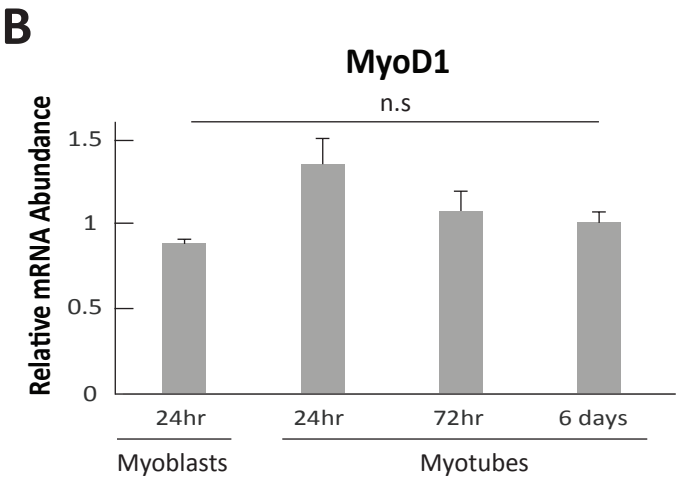
B
MyoD1
n.s
Relative mRNA Abundance
1.5
1
0.5
0
24hr
24hr
72hr
6 days
Myoblasts
Myotubes

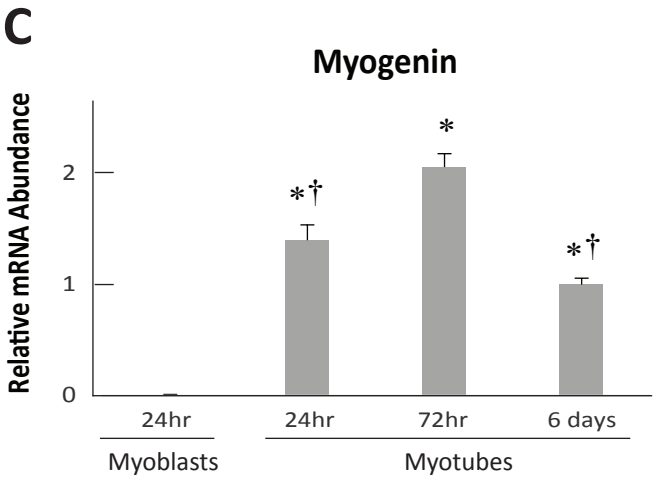
C
Myogenin
Relative mRNA Abundance
2
1
0
*†
*
*†
24hr
24hr
72hr
6 days
Myoblasts
Myotubes

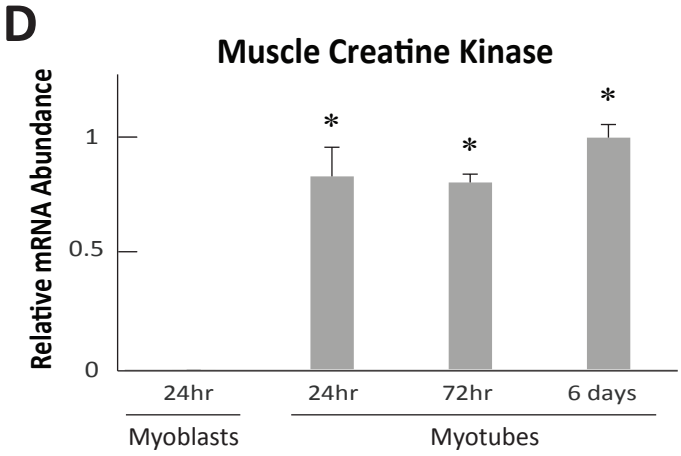
D
Muscle Creatine Kinase
Relative mRNA Abundance
1
0.5
0
*
*
*
24hr
24hr
72hr
6 days
Myoblasts
Myotubes

Figure 4 (continued)

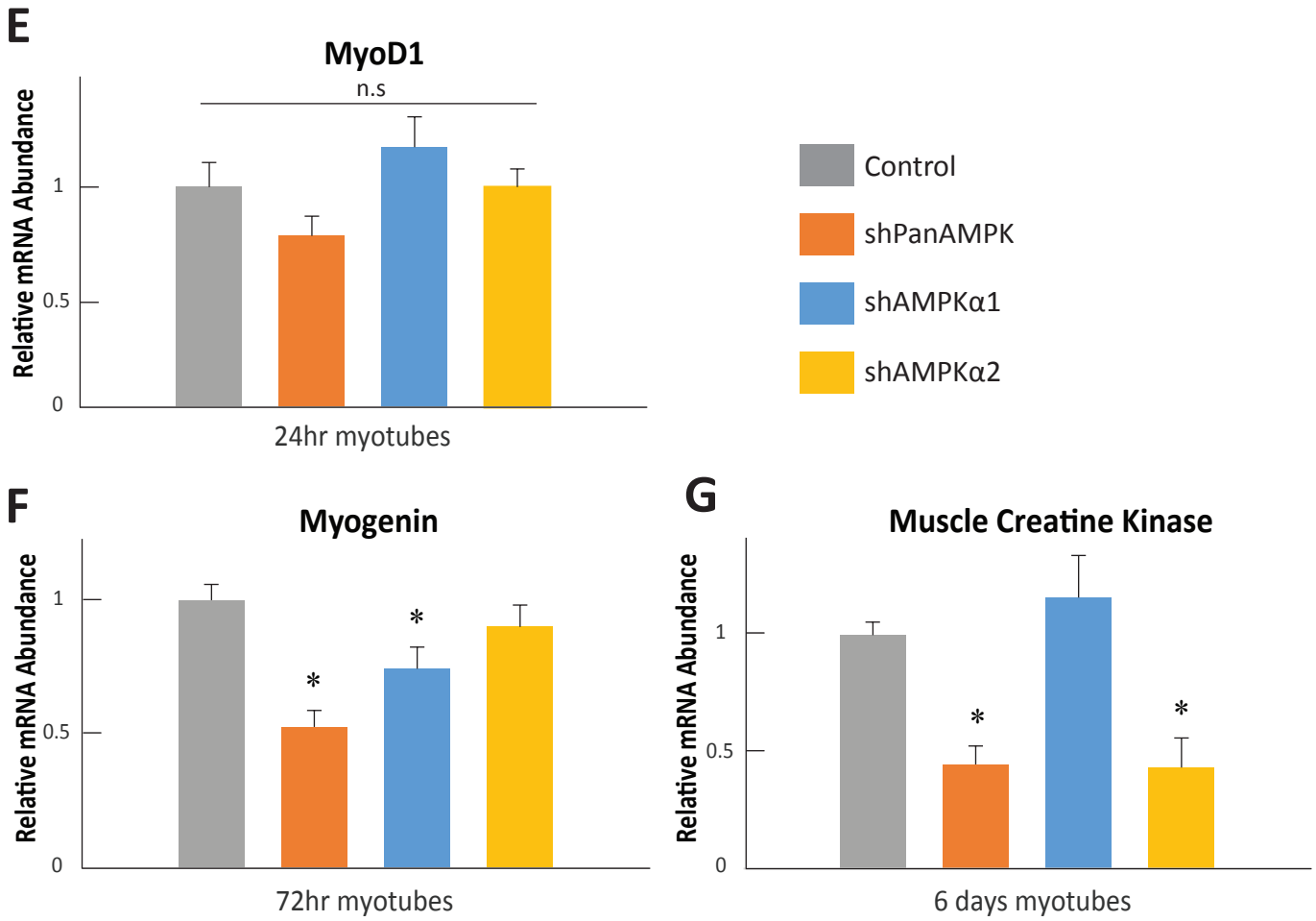

Figure 5

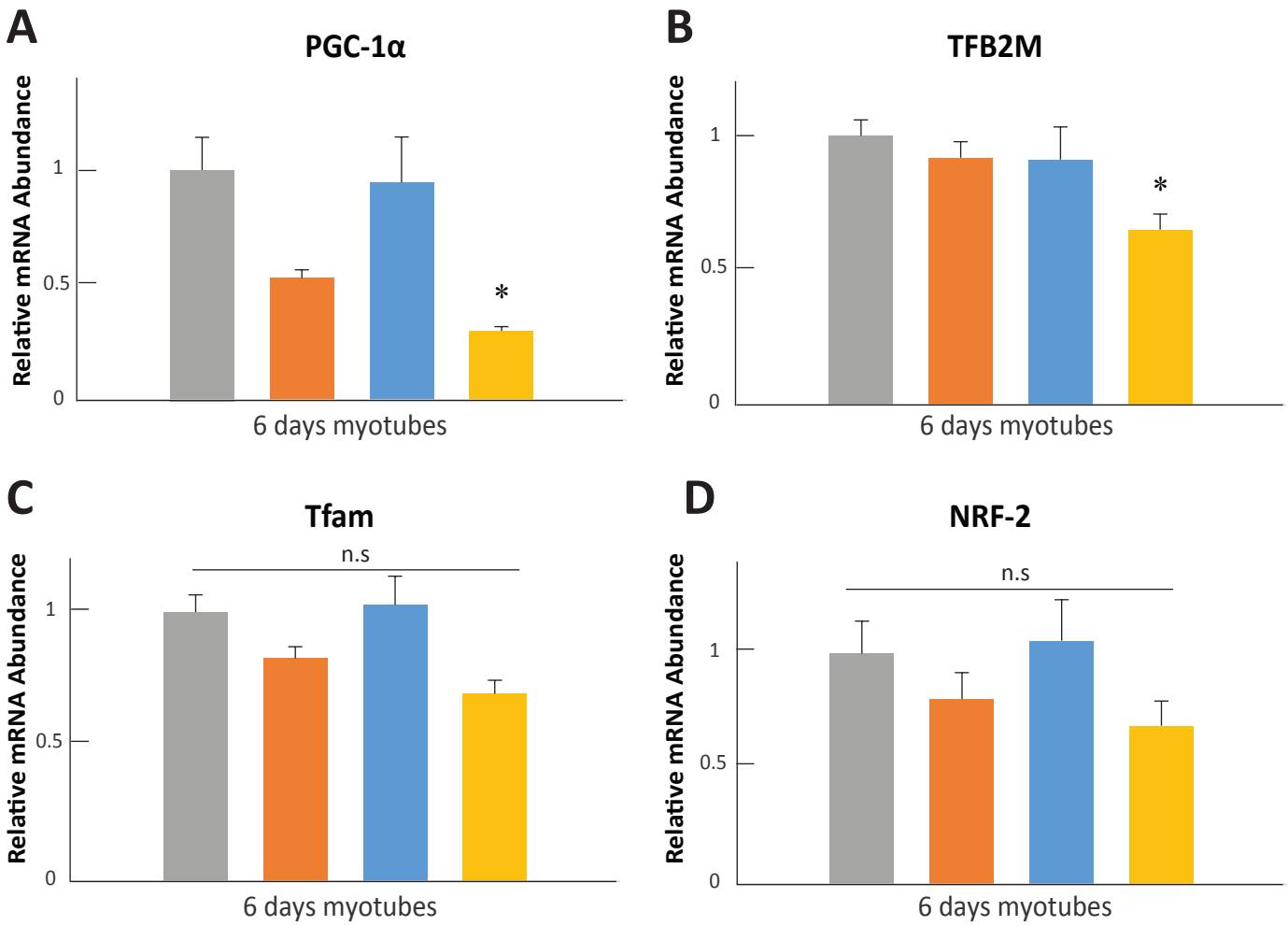
A
PGC-1α
Relative mRNA Abundance
1
0.5
0
*
6 days myotubes
B
TFB2M
Relative mRNA Abundance
1
0.5
0
*
6 days myotubes
C
Tfam
n.s
Relative mRNA Abundance
1
0.5
0
6 days myotubes
D
NRF-2
n.s
Relative mRNA Abundance
1
0.5
0
6 days myotubes

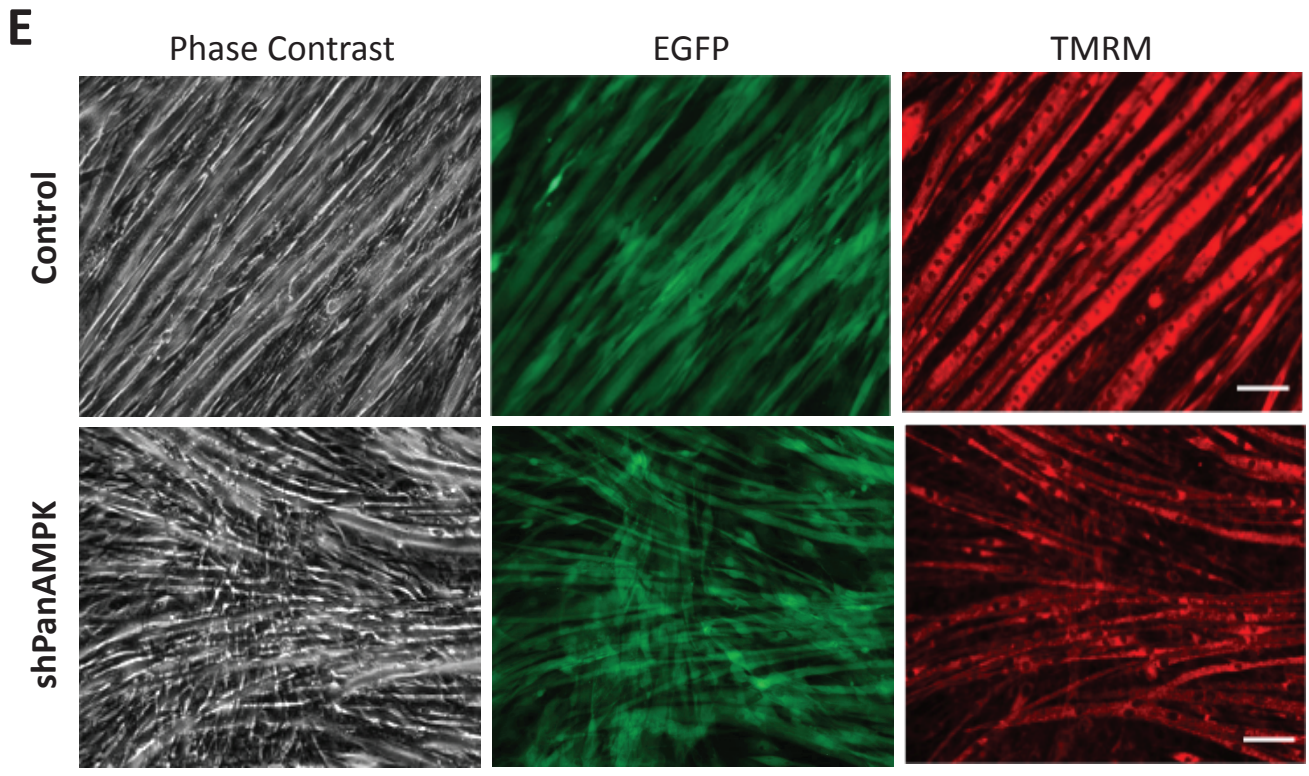
E
Phase Contrast
EGFP
TMRM
Control
shPanAMPK

Figure 5 (continued)

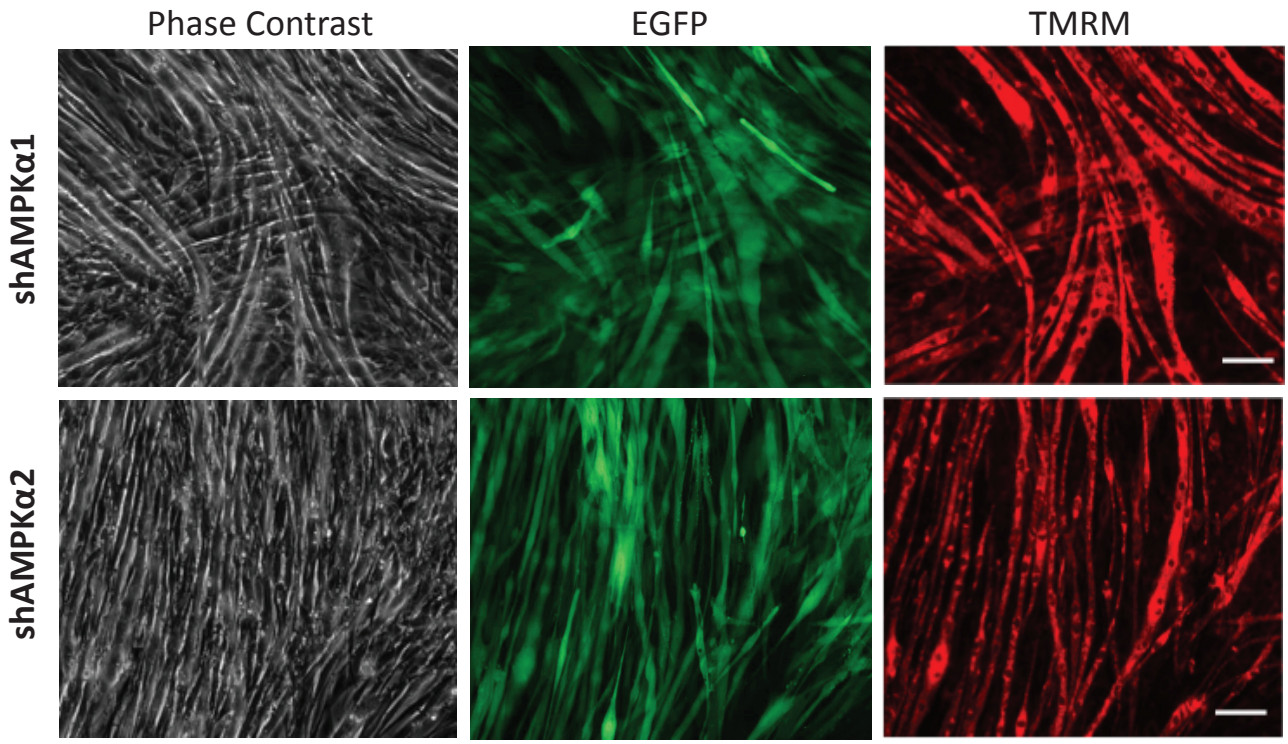

F

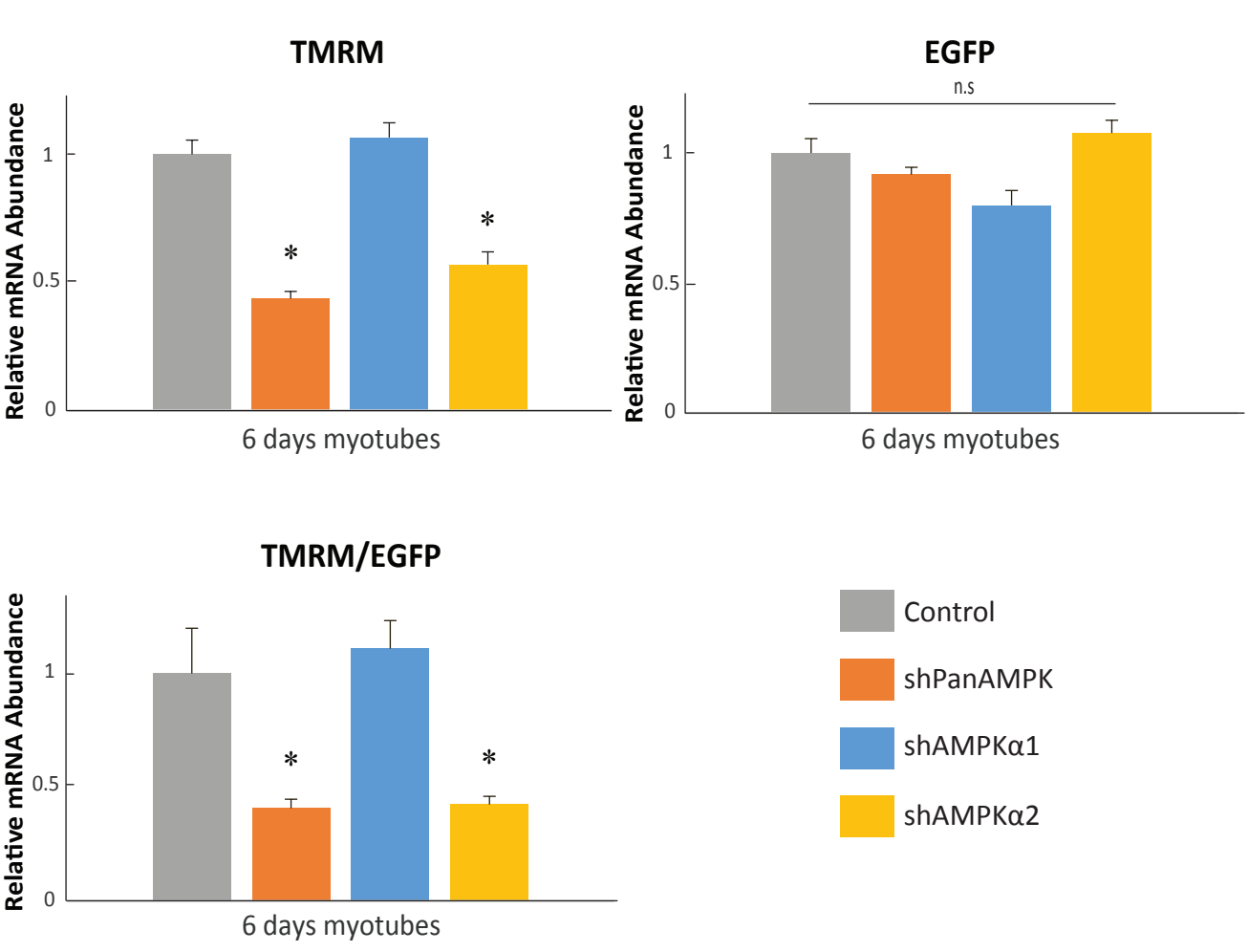

Figure 6

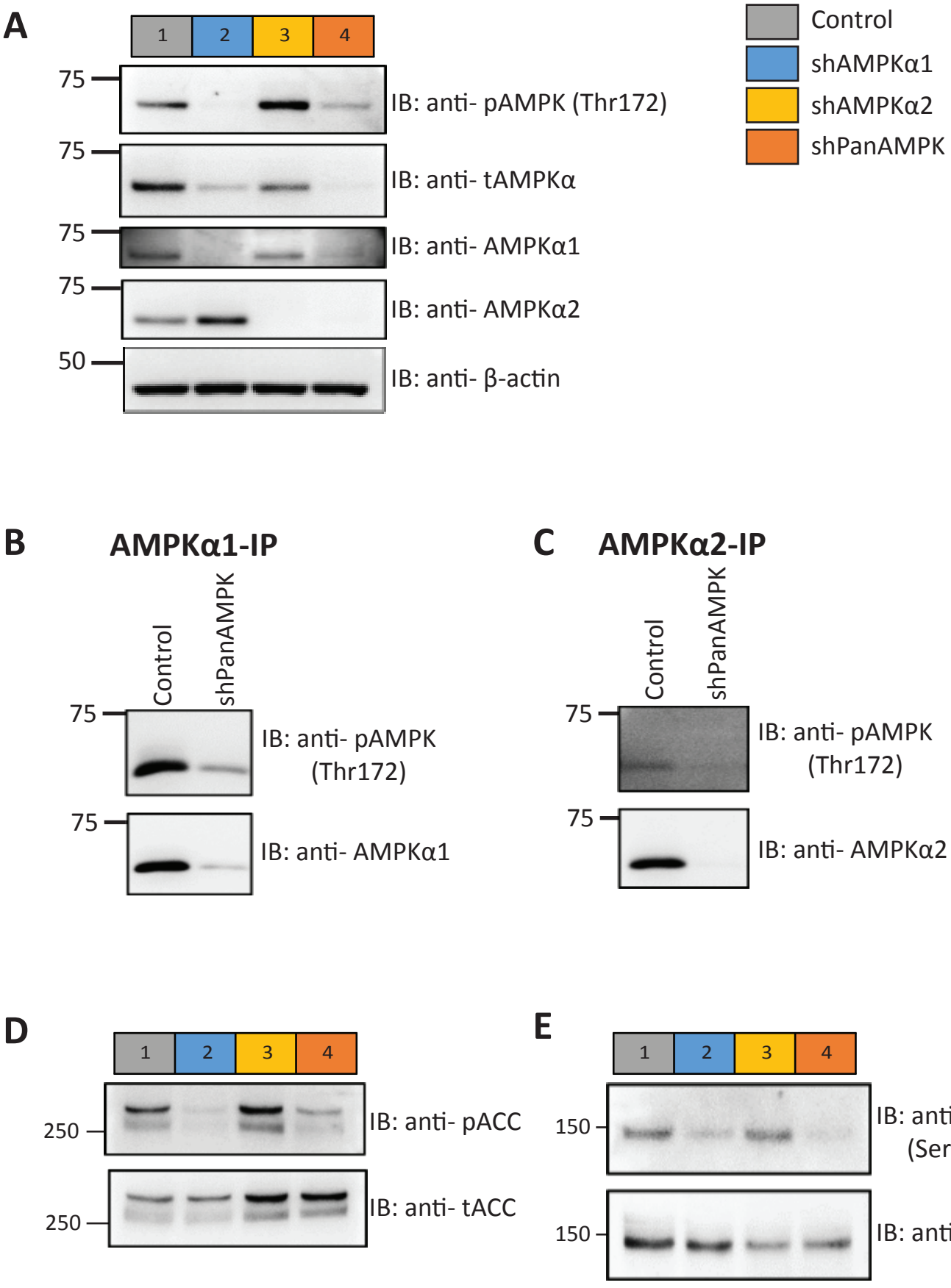
A
1
2
3
4
Control
shAMPKα1
shAMPKα2
shPanAMPK
75
IB: anti- pAMPK (Thr172)
75
IB: anti- tAMPKα
75
IB: anti- AMPKα1
75
IB: anti- AMPKα2
50
IB: anti- β-actin
B
AMPKα1-IP
Control
shPanAMPK
75
IB: anti- pAMPK (Thr172)
75
IB: anti- AMPKα1
C
AMPKα2-IP
Control
shPanAMPK
75
IB: anti- pAMPK (Thr172)
75
IB: anti- AMPKα2
D
1
2
3
4
250
IB: anti- pACC
250
IB: anti- tACC
E
1
2
3
4
150
IB: anti- pULK1 (Ser555)
150
IB: anti- tULK1

Figure 7

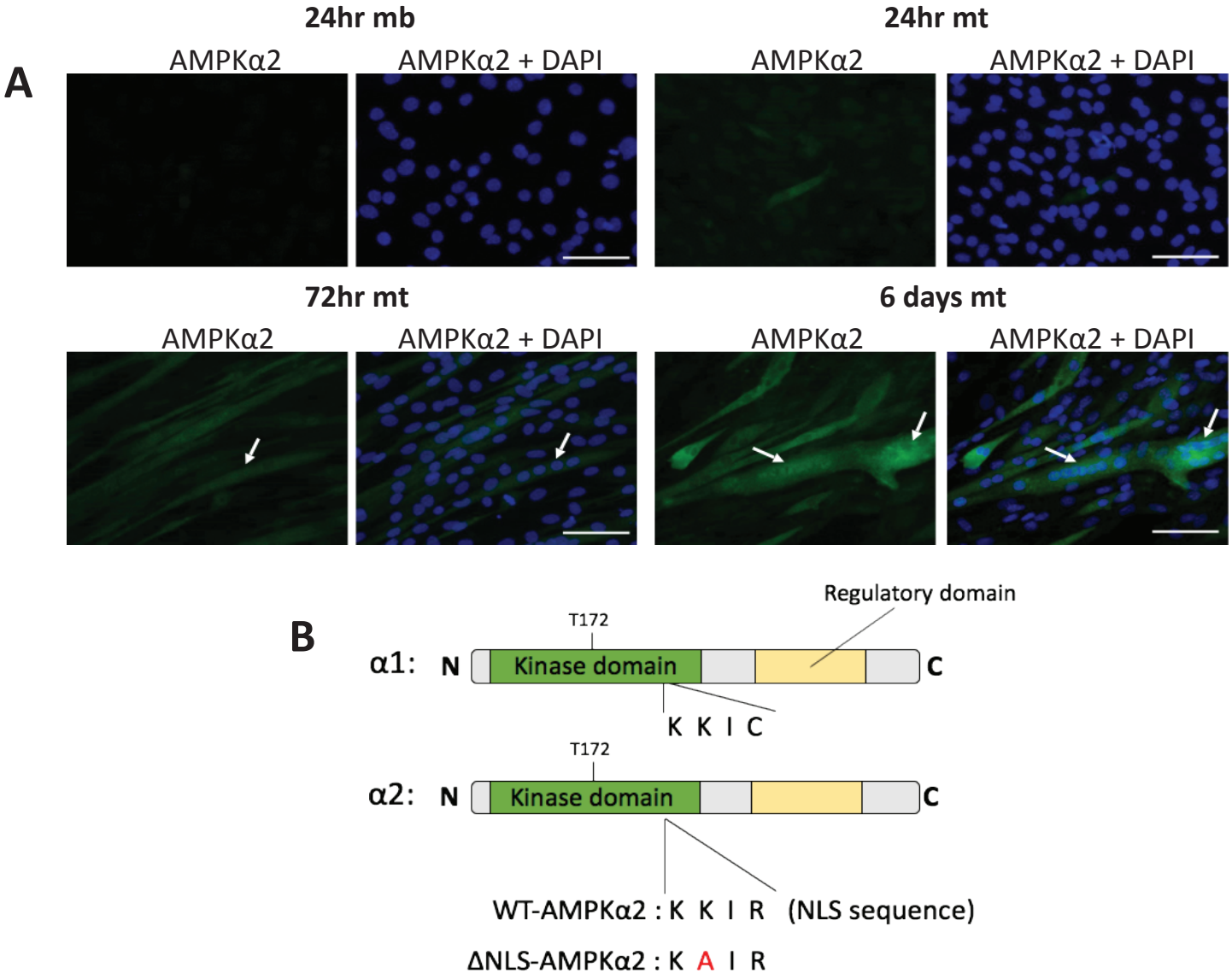
A
24hr mb
AMPKα2
AMPKα2 + DAPI
24hr mt
AMPKα2
AMPKα2 + DAPI
72hr mt
AMPKα2
AMPKα2 + DAPI
6 days mt
AMPKα2
AMPKα2 + DAPI
B
Regulatory domain
T172
α1: N
Kinase domain
C
K K I C
T172
α2: N
Kinase domain
C
WT-AMPKα2 : K K I R (NLS sequence)
ΔNLS-AMPKα2 : K A I R
C
WT-AMPKα2
ΔNLS-AMPKα2
Control
AICAR

Figure 7 (continued)

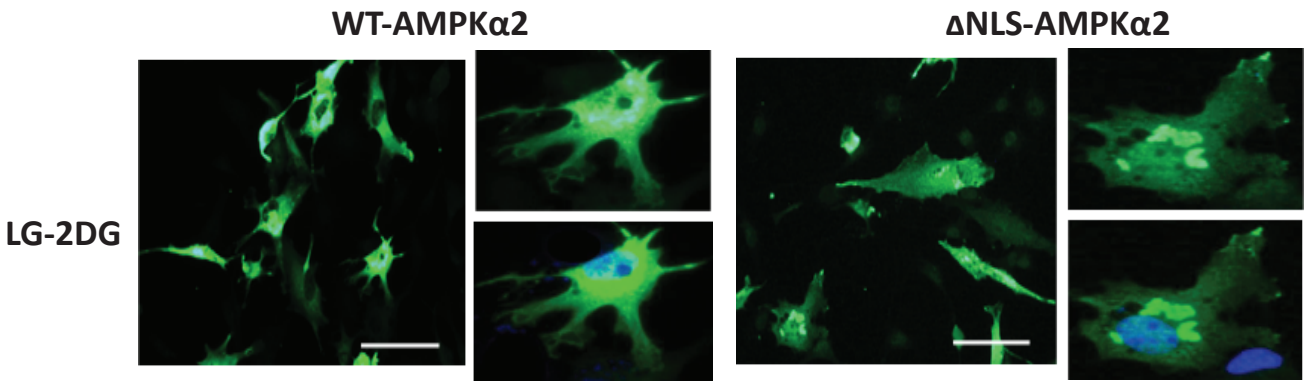

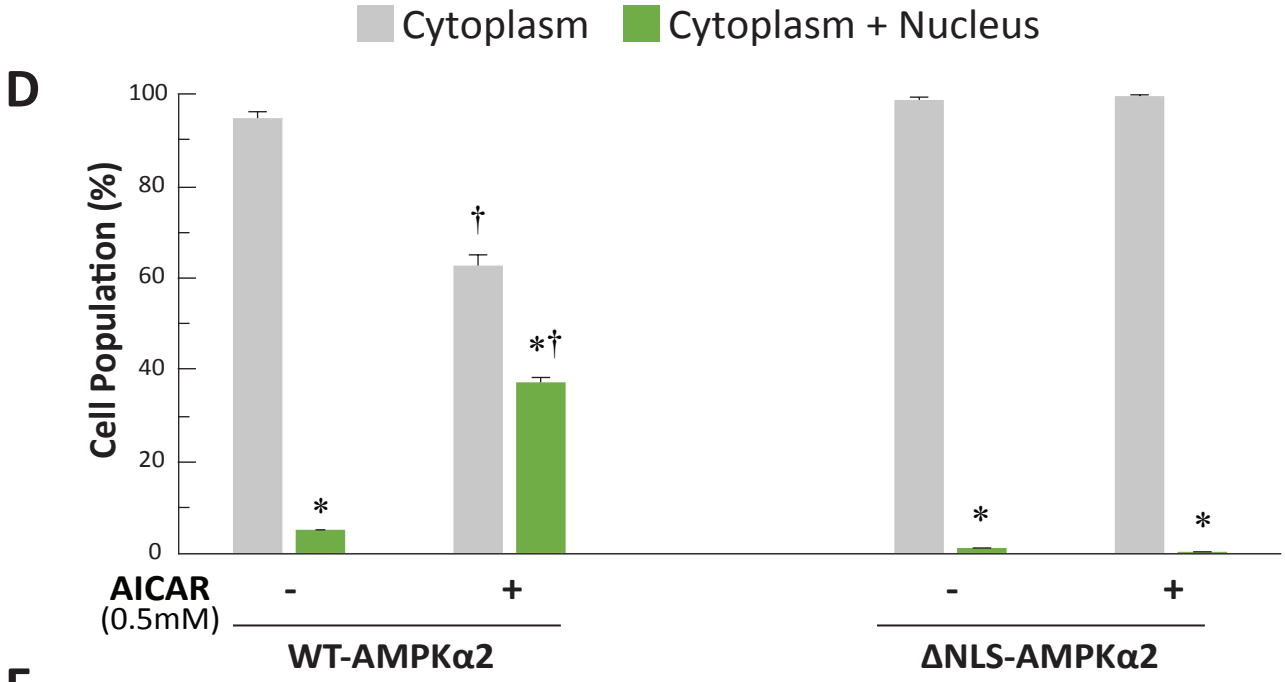

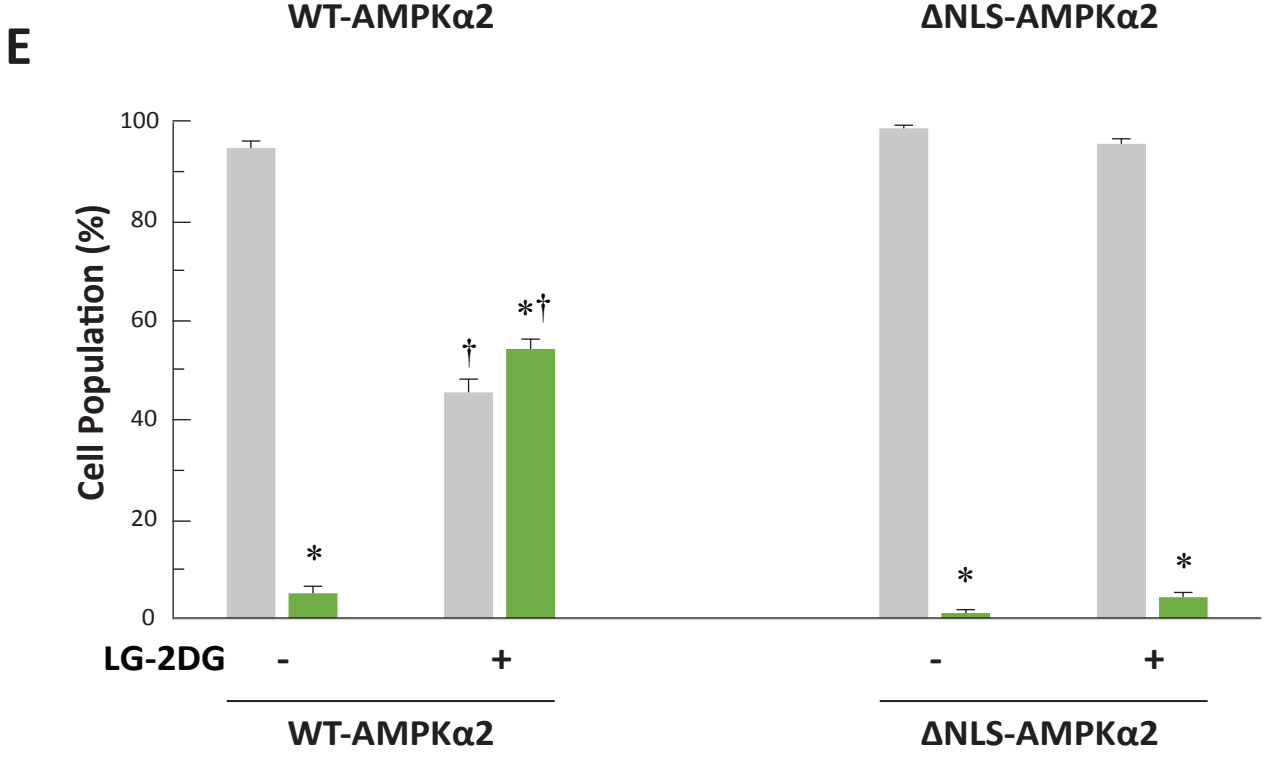

Figure 8

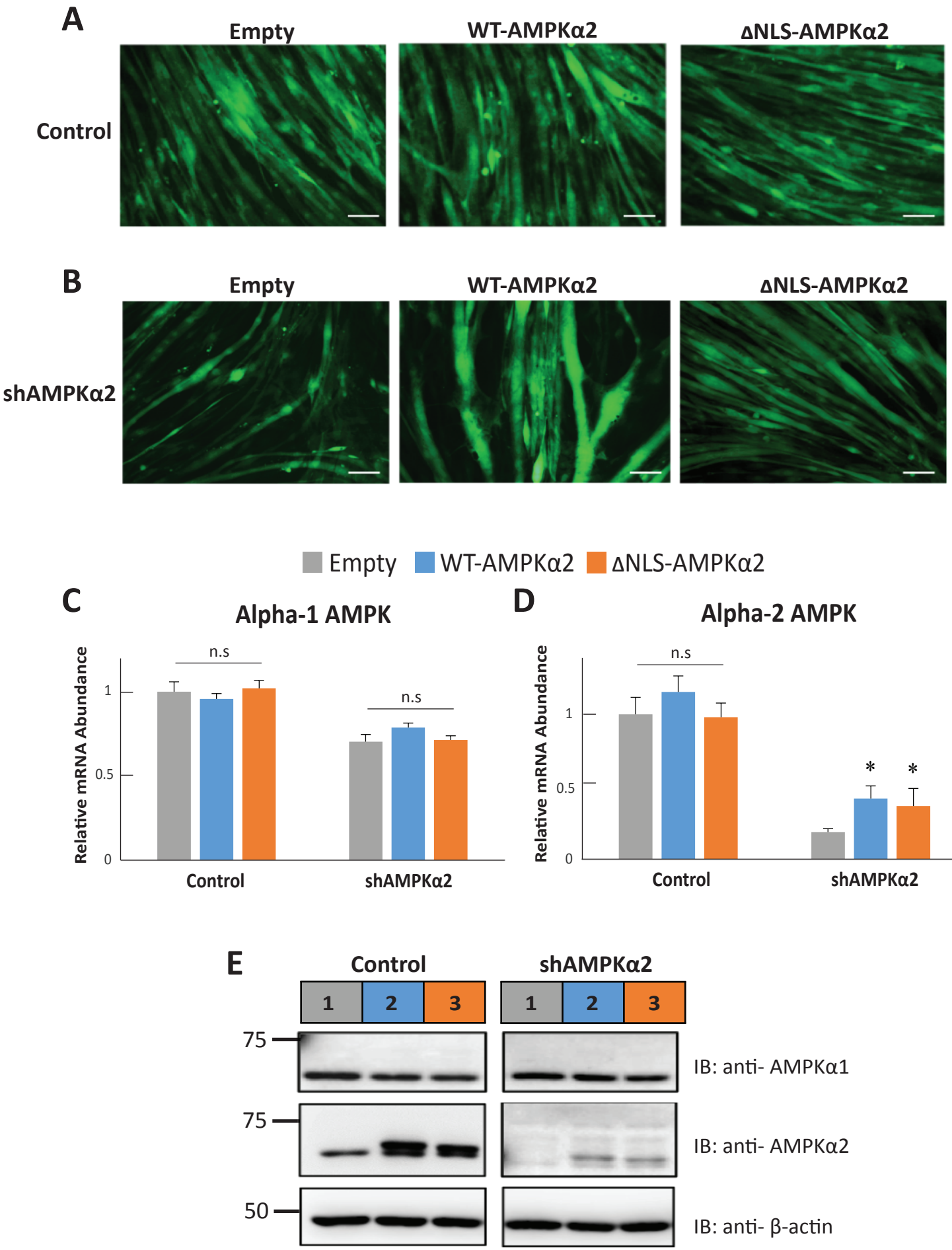
A
Empty
WT-AMPKα2
ΔNLS-AMPKα2
Control
B
Empty
WT-AMPKα2
ΔNLS-AMPKα2
shAMPKα2
Empty
WT-AMPKα2
ΔNLS-AMPKα2
C
Alpha-1 AMPK
Relative mRNA Abundance
n.s
n.s
1
0.5
0
Control
shAMPKα2
D
Alpha-2 AMPK
Relative mRNA Abundance
n.s
*
*
1
0.5
0
Control
shAMPKα2
E
Control
shAMPKα2
1
2
3
1
2
3
75
75
50
IB: anti- AMPKα1
IB: anti- AMPKα2
IB: anti- β-actin

Figure 8 (continued)

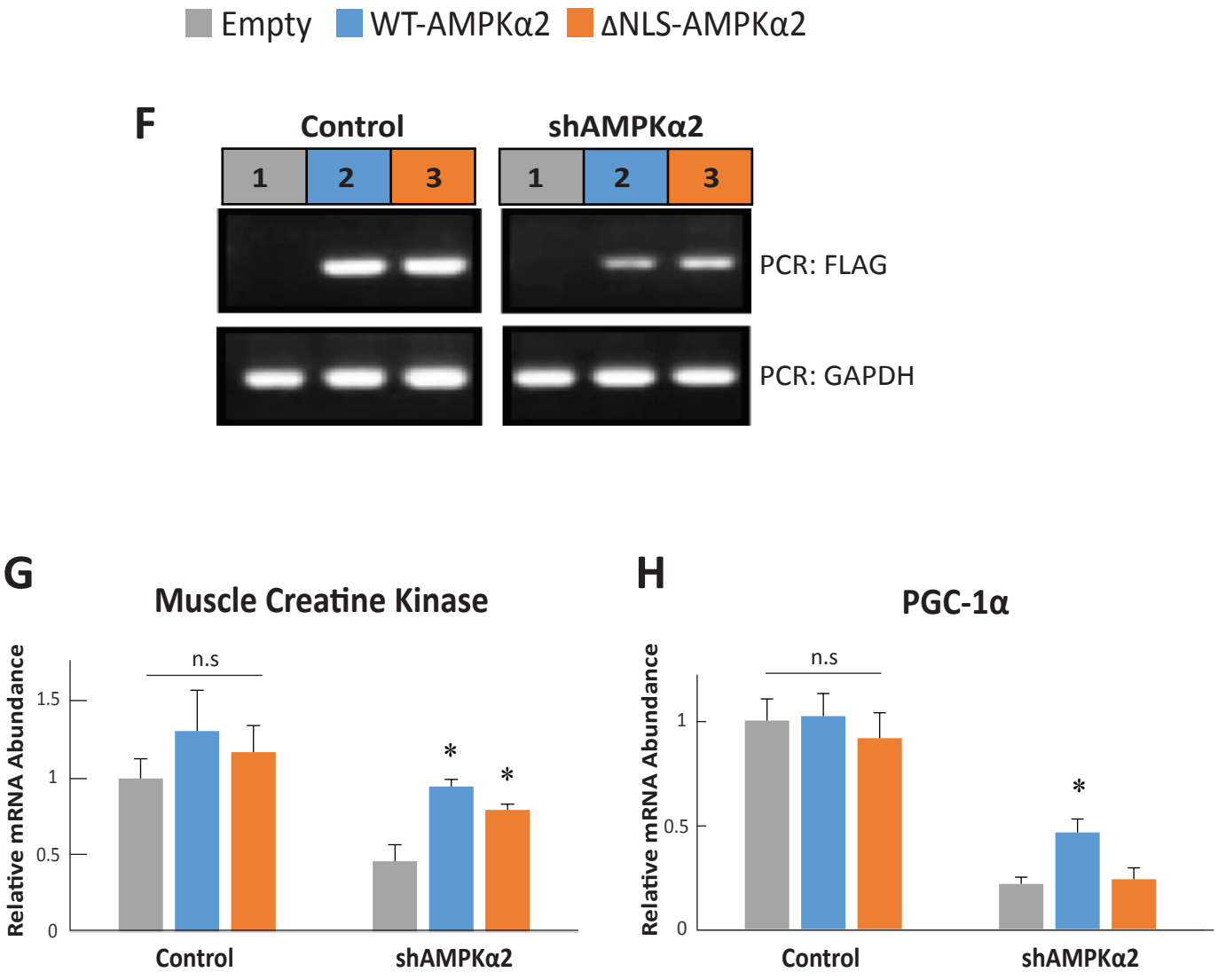

Figure 9

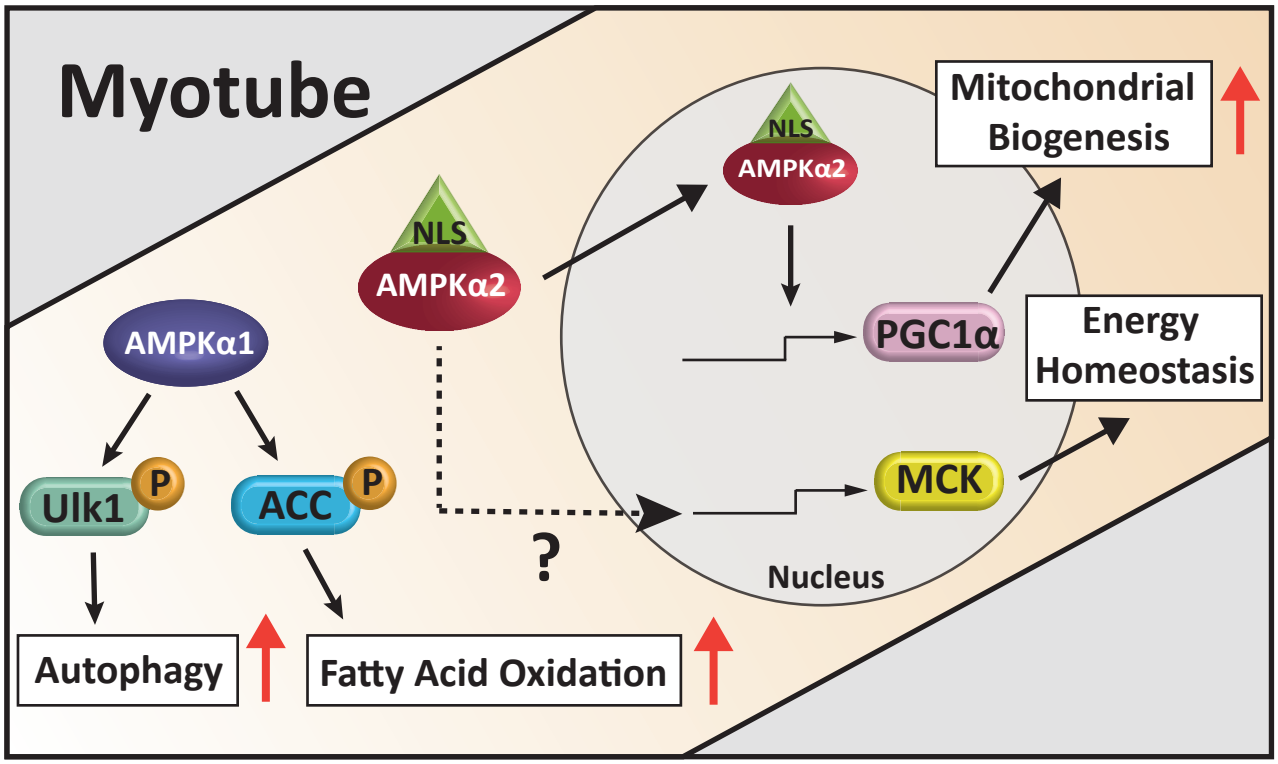
Myotube
NLS
AMPKα2
NLS
AMPKα2
Mitochondrial Biogenesis
AMPKα1
PGC1α
Energy Homeostasis
Ulk1
P
ACC
P
MCK
?
Nucleus
Autophagy
Fatty Acid Oxidation